Title
Development of Diverse Cardiovascular Structures Derived from the Second Heart Field

Author
Harmon, Andrew William

Publication Date
2014

Peer reviewed|Thesis/dissertation

UNIVERSITY OF CALIFORNIA

Los Angeles

Development of Diverse Cardiovascular Structures Derived from the Second Heart Field

A dissertation submitted in partial satisfaction

of the requirements for the degree

Doctor of Philosophy in Molecular, Cell and Developmental Biology

by

Andrew William Harmon

2014

ABSTRACT OF THE DISSERTATION

Development of Diverse Cardiovascular Structures Derived from the Second Heart Field

by

Andrew William Harmon

Doctor of Philosophy in Molecular, Cell and Developmental Biology

University of California, Los Angeles, 2014

Professor Atsushi Nakano, Chair

The heart is a specialized organ, responsible for distributing oxygenated blood through long distances of systemic vasculature. When fully formed it is composed of diverse cells types from several embryonic origins that must coordinate in order to function properly. During mammalian development the heart is the first organ to form and must become fully functional prior to the completion of organogenesis. The migratory cardiac progenitor population known as the second heart field is responsible for contributing not only additional cardiomyocytes to the nascent heart, but also endothelial and smooth muscle cells that will develop into specialized structures. Although the fates of the SHF have been well described, many potential mechanisms regulating the development of tissue derived from these progenitors remain to be examined.

This thesis is composed of five chapters including three original research articles (one of which has been published) and one that describes a recently established project. Chapter One will serve as an introduction and overview of heart development and cardiac-stem cell biology, including the cell fates of FHF and SHF progenitors. The contribution SHF-progenitors to the ascending aorta and the anatomical boundaries of the tissue derived from this source will be discussed in Chapter Two: "Nkx2-5 lineage tracing visualizes the distribution of second heart field-derived aortic smooth muscle". The role of the Serum Response Factor (SRF) co-factor Myocardin (Myocd) within the embryonic heart and SHF-derived smooth muscle will be described in Chapter Three: "The Role of Myocardin in Cardiogenesis and the Development SHF-derived Smooth Muscle". Finally, the role of inhibitory Smad (iSmad) proteins in the formation of SHF-derived cardiac structures will be discussed in Chapter Four: "The Role of Inhibitory Smads in the Embryonic Heart". The last chapter will discuss conclusions, implications of this work and future directions.

The dissertation of Andrew William Harmon is approved.

Jau-nian Chen

Karen Lyons

April Pyle

Atsushi Nakano, Committee Chair

University of California, Los Angeles

2014

This dissertation is dedicated to Heidi,

my original scientific role model

Table of Contents

LIST OF FIGURES

CHAPTER 2

CHAPTER 3

CHAPTER 4

ACKNOLEDGEMENTS

I would first and foremost like to thank my advisor Dr. Atsushi Nakano for giving me the opportunity to perform my dissertation work in his lab. I am grateful that I was able to work in an environment that fostered my growth as a researcher and that as the first student in his lab we were able to navigate the graduate school process together. I also appreciate that he encouraged me to approach many questions independently, but was always available to give me guidance in any and all facets of the scientific process.

I would also like to thank my committee members Dr. Karen Lyons, Dr. Jau-nian Chen and Dr. April Pyle for their time, support and advice. Their expertise and feedback during the manuscript re-submission process was especially valuable as well as motivating. I would also like to thank Dr. Lyons for allowing me to TA for her and being an excellent role model as an educator in the life sciences.

I would like to acknowledge all my present and past colleagues from the Nakano laboratory for their friendship and support during my time at UCLA. Specifically I would like to recognize Haruko for her continued effort as the laboratory's manager and keeping the lab running smoothly while juggling the duties of a post-doctoral researcher. Star Williams for her friendship and help when I first joined the laboratory as well as Jane and Rana for their dedication, hard work and patience as my undergraduate protégés. I am also grateful for Yas's keen experimental eye and Gentian's near encyclopedic knowledge of cardiac anatomy, development and malignancies.

I would like to thank the members of the CMB training program, in particular Dr. Steven Clarke for his enthusiasm, perspective and dedication to graduate training. Also Christine

Briganti for her tireless work as the student affairs officer of the program and as a model of administrative effectiveness.

I would like to thank my friends and family for all their support and encouragement. In particular I will always be grateful to Matt Veldman for his mentorship and support. Matt is a rare researcher who elevates the work and potential of everyone around him. He was always willing to lend his expertise no matter how big or trivial the question and I feel lucky to call him a close friend and scientific confidant. Finally, I would like to express unending appreciation for Katrina, for helping to make me a better scientist and more importantly a better person.

Chapter Two of this dissertation is a re-print of "Nkx2-5 lineage tracing visualizes the distribution of second heart field-derived aortic smooth muscle" from *Genesis* Volume 51, Pages 862-869 with permission from John Wiley and Sons.

This work was supported by pre-doctoral fellowships awarded through the National Institutes of Health – Ruth L. Kirschstein National Research Service Award, GM007185, as well as the UCLA Fred Eiserling and Judith Lengyel Graduate Doctorate Fellowship in the Life Sciences.

VITA

2008	Honors Bachelor of Science with Distinction Biological Sciences Concentration in Cell and Molecular Biology and Genetics University of Delaware
2010 – 2013	Teaching Assistant Dept. of Molecular, Cell and Developmental Biology University of California, Los Angeles

PUBLICATIONS

Harmon A.W. and Nakano A. Nkx2-5 lineage tracing visualizes the distribution of second heart field-derived aortic smooth muscle. *Genesis* 51, 862-869 (2013)

Nakano H., Liu X., Arshi A., Nakashima Y., van Handel B., Sasidharan R., **Harmon A.W.**, Shin J.H., Schwartz R.J., Conway S.J., Harvey R.P., Pashmforoush M., Mikkola H.K., Nakano A. *Nature Communications* 4, 1564 (2013)

CHAPTER ONE:

Introduction

1. Development of the Mammalian Heart

The heart is a specialized organ, responsible for distributing oxygenated blood through long distances of systemic vasculature. When fully formed it is composed of diverse cells types from several embryonic origins that must coordinate in order to function properly. During mammalian embryogenesis the heart is the first organ to form and must become fully functional as a linear heart tube, prior to the completion of organogenesis and its maturation into a complex four-chambered pump. This Chapter will focus on the early stages of heart development as they pertain to the migration and differentiation of second heart field progenitors and the tissue derived from these cells.

1.1 Early Events

The formation of the heart begins with the ingression of Brachury (Bry) positive mesoderm through the primitive streak. After completing ingression early in gastrulation at mouse embryonic day (E) 6.5, a subset of these progenitors migrates away from the primitive streak in an anterior-lateral fashion (Yang et al., 2002; Showell et al., 2004). This migration relies upon the down-regulation of Bry and up-regulation of Mesoderm Posterior 1 (Mesp1). Mesp1 is responsible for initiating a cardiogenic gene program and further restricting mesodermal progenitors to a cardiac fate (Martin-Puig et al., 2008). The $Mesp1^{+}$ cardiogenic mesoderm localizes into two bi-lateral populations of progenitors within the ventral splanchnic layer of the lateral plate mesoderm (Saga et al., 1999). These populations, referred to as the heart fields, will form a continuous cardiac crescent by E7.5. At this stage two distinct populations of cardiac progenitors can be observed by molecular markers, the First Heart Field (FHF), which makes up

the ventral portion of the crescent and the Second Heart Field (SHF), which lays dorsal and medial to the FHF.

It is worth noting that controversy remains concerning whether these two populations of "heart fields" represent truly independent progenitors or merely subsets of the same cardiogenic field. An alternative model suggests that the heart arises from a single organ field comprised of a homogenous population of cardiac progenitors. Accordingly, the FHF and SHF may represent a "progressive restriction of developmental potency" due to differential exposure to signaling factors (Moorman et al., 2007). While consensus has not been reached, here we will use the FHF and SHF nomenclature to describe the two main sub-populations of progenitor cells distinguished within the cardiac crescent.

At E8.0 the arms of the cardiac crescent migrate to the ventral midline and fuse together to form the linear heart tube derived from the FHF. The nascent heart is made up of an outer myocardial layer and an inner endothelial layer called endocardium. At this point the heart tube begins to beat and must maintain fetal blood circulation to and from the placenta, while simultaneously undergoing the rest of its development. Subsequent to the formation of the linear heart, looping then occurs at E8.5 (Zaffran et al., 2004). During this process the heart tube, which is originally aligned with the midline, undergoes ventral bending, creating the ventricular bend, followed by rightward rotation (Männer, 2000). The "C" shaped loop then undergoes further morphological re-arrangement, during which the outflow and inflow connections to the dorsal body wall are moved closer together, and the inflow tract and future atrium are raised cranially so that they are now above the future common ventricle (Taber et al., 1995). This arrangement then prepares the heart for subsequent maturation into a four-chambered morphology.

1.2 The First and Second Heart Field

The first evidence of a so-called second heart field was seen in chick and described the formation of the outflow tract from tissue outside of the cardiac crescent (now referred to as the FHF) (Liebman, 1976). Using a variety of molecular markers, heart development can now be described through the contribution of specific multipotent progenitor populations, including the FHF and SHF.

Recent embryonic stem (ES) cell studies have described a multipotent cardiac progenitor population analogous to the initial cardiac field present in the splanchnic mesoderm. These common cardiac progenitors are marked by expression of Flk1/Isl1/Nkx2-5 and are capable of differentiation into cardiomyocytes, endothelial cells and smooth muscle (Kattman et al., 2006; Moretti et al., 2006; Wu et al., 2006). As the cardiac crescent forms at E7.0 common cardiac progenitors lose expression of Flk1, it is at this point that the FHF also ceases expression of Isl1, allowing the SHF to be identified molecularly through the continued expression of this transcription factor (Nakano 2008). Within the cardiac crescent, the FHF is located ventrally and laterally to the SHF, resulting in exposure to key developmental signaling molecules, including: Wnt antagonists, Bone Morphogenetic Protein (BMP) and Fibroblast Growth Factor (FGF). The result is expression of lineage specific regulators of cardiac fate in the FHF, specifically: Nkx2-5, Gata-4 and T-box Transcription Factor 5 (Tbx5). Subsequently, the FHF begins to commit to a cardiomyocyte fate and initiates expression of contractile proteins such as myosin light chain-2a (Mlc2a), myosin light chain-2v (Mlc2v) and myosin heavy chain (Mhc) (Brade et al., 2013). The cells of the FHF will begin differentiation within the cardiac crescent just prior to formation of the linear heart tube. This allows cardiac progenitor populations to be

further distinguished, as the FHF can now be visualized by markers of differentiated cardiomyocytes such as Mlc2a (Cai et al., 2003).

As the FHF-derived heart tube forms and moves into the pericardial space, the SHF progenitor population continues to reside within the dorsal pericardial wall, physically separated from the nascent heart except at the inflow and outflow tract connections (Kelly et al., 2001). During the formation of the heart tube, progenitors of the SHF will remain undifferentiated and continue to proliferate. Given that cardiomyocytes within the FHF-derived heart tube exhibit extremely low cell division rates, the subsequent elongation of the heart is accomplished by the acquisition of migratory SHF progenitor cells (van den Berg et al., 2009). In order to enter the heart, which is separated from the ventral body wall, SHF progenitors migrate through the pharyngeal mesoderm into both the anterior and posterior poles of the developing organ (van den Berg et al., 2009). This migration begins concurrently with heart looping and is also when the common SHF progenitor population, marked by $Isl1^{+}/Nkx2\text{-}5^{+}$, can be further classified as anterior SHF progenitors or posterior SHF progenitors based on which pole they migrate through to enter the heart.

Despite migrating from a common progenitor population that does not exhibit any physical separation, the anterior and posterior SHF can be distinguished, in part, by molecular markers. Expression of myocyte-specific enhancer factor-2c (Mef2c) distinguishes the identity of the anterior SHF (Verzi et al., 2005). While there are presently no markers of the early posterior SHF, expression of the sarcomeric protein Sarcolipin (Sln) identifies further differentiated atrial progenitors derived from the posterior SHF (Nakano et al., 2011).

The progenitor cells of the anterior SHF invade the arterial pole of the heart tube, down-regulating progenitor markers such as Isl1, and contributing cardiomyocytes to the portion of the

looped heart that will become the future right ventricle. Additionally, these progenitors supply both cardiac and smooth muscle to the developing outflow tract. This specific cardiomyocyte contribution has immediate morphological consequences, as it is responsible for the immediate elongation of the linear heart tube from the anterior pole during the initiation of heart looping (Cai et al., 2003; Kelly et al., 2001). The contribution of the SHF to aortic smooth muscle was first described in chick (Waldo et al., 2005). In this model, as looping commences the initial FHF-derived outflow tract (conus) is present directly cranial to the right ventricle. Early migratory anterior SHF cells will add an additional segment of outflow myocardium (truncus), while later migrating anterior SHF cells will comprise the smooth muscle of the aortic base and pulmonary trunk. Therefore, the cells that comprise the transition from beating cardiac muscle to the smooth muscle of the great arteries originate from the same SHF population, but most likely are determined before migration (Waldo et al., 2005).

The progenitors of the posterior SHF will migrate via the future venous pole of the heart and invade the inflow tract and future atria. The differentiated posterior SHF will ultimately give rise to the majority of cardiomyocytes within both atria as well as the myocardial sleeves that envelope the great veins as they enter the heart (Sun et al., 2007). Additionally, recent evidence suggests that late-stage atrial progenitors exhibit smooth muscle plasticity *ex vivo* and contribute a modest number of smooth muscle cells within the sinus venosus (Nakano et al., 2011).

While the diverse fates of the second heart field have been well described, important questions remain concerning what regulates the formation of SHF-derived smooth muscle and its relationship with surrounding cardiovascular tissue. In Chapter Two the anatomical distribution of SHF-derived smooth muscle will be described in new detail. Our studies will look at the distribution of SHF-derived smooth muscle in the aortic base in the context of cell populations

surrounding this tissue. Specifically, we will describe the formation of a vertical boundary between SHF and Neural Crest Cell (NCC)-derived smooth muscle within the ascending aorta and the clinical implications of this region. In Chapter Three we investigate whether common signaling systems regulate the two types of muscle that arise from the anterior SHF. Specifically, we will show a differential requirement for the Serum Response Factor (SRF) co-factor Myocardin (Myocd) in the maturation of cardiac versus smooth muscle.

2. Development of the Coronary Vasculature

During early cardiogenesis, the primitive heart tube is thin walled and nascent cardiomyocytes are supplied with oxygen through simple diffusion via the blood that is pumped through the endocardial-lined lumen. As the mammalian heart continues to develop and the myocardium thickens, simple diffusion is no longer an adequate method of oxygenation (Lluri and Aboulhosn, 2014). The coronary vasculature therefore represents a critical step in heart development and a major source of cardiac disease, as it is responsible for supplying oxygenated blood back into the working myocardium of the heart. While there is generally consensus over the origin of coronary smooth muscle, the origin and development of coronary endothelial cells remains controversial (Del Monte and Harvey, 2012).

2.1 Coronary Endothelium

Historically it has been believed that the majority of the coronary endothelium arises from the pro-epicardium and by *de novo* vasculogenesis. This model originated from the finding that ablation of the epicardium resulted in a complete lack of coronary vasculature (Liebman, 1976).

At E9.5 the pro-epicardial organ attaches to the dorsal wall of the naked heart tube and begins to spread over the organ as a single mesothelial layer. By E11.5 the entire heart is encapsulated by the epithelial sheet of the epicardium (Komiyama et al., 1987). Subsequently a subset of cells within the epicardium will undergo epithelial to mesenchymal transition (EMT) and move into the sub-epicardial space as epicardium-derived cells (EPDCs). These EPDCs then differentiate into endothelial cells within the sub-epicardium, then undergo vasculogenesis forming a coronary plexus that completely covers the ventricles by E13.5. After plexus formation the coronary endothelium undergoes remodeling and additional angiogenesis. In this model the coronary vasculature is completely independent of the systemic circulation until approximately E14.5, at this time the coronary arteries connect to the base of the aorta, establishing the coronary circulation (Mikawa and Gourdie, 1996; Pérez-Pomares et al., 2002).

However, this dogma has been called into question by recent lineage tracing experiments that have proposed novel origins for the coronary vasculature. The use of an *Apelin*-nLacZ knock-in line, in combination with labeled organ culture models, has suggested that the coronary vasculature originates through angiogenesis and reprogramming of previously established endothelial cells within the sinus venosus (Red-Horse et al., 2010). Interestingly, under this model the coronary vasculature is continuous with the systemic circulation throughout its inception, but the cardiac vascular circuit would not be complete until the connection of the vessels with the aortic base.

A third model utilizes Nuclear Factor of Activated T-cells 1 (NFATC1) to suggest that it is the endocardium itself that is the source of the coronary arteries (Wu et al., 2012). This molecular marker is proposed to specifically mark the endocardium and is not expressed within the pro-epicardium or the coronary endothelium once it is formed. Within this model a subset of

endocardial cells down-regulate NFATC1 starting at E11.5, go through EMT and invade the myocardial wall in response to a VEGF gradient secreted from working cardiomyocytes. Vasculogenesis will then occur in a similar vision to what had been initially described for EPDCs.

2.2 Coronary Smooth Muscle

Similar to the mechanism originally believed to describe formation of the coronary endothelium, coronary smooth muscle is mainly derived from cells of the epicardium that have undergone EMT and migrated into the sub-epicardial space (Pérez-Pomares et al., 2002). The pro-epicardial organ, and thus the majority of coronary smooth muscle, can be traced back to both the FHF and SHF (Zhou et al., 2008). However, lineage tracing with the neural crest marker Wnt1 demonstrates that smooth muscle surrounding the main coronary arteries, adjacent to the aortic cusps, is derived from a non-cardiac progenitor source (Jiang et al., 2000).

While the source of coronary smooth muscle is agreed upon within the vascular biology field, the interaction between epicardium and neural crest cell-derived cells within the main coronary arteries has previously not been examined. Chapter 2 will specifically show that coronary smooth muscle proximal to the aorta does not represent a unique neural crest-derived compartment. Rather, proximal coronaries contain a mixture of smooth muscle from both neural crest and cardiac progenitor origins without a strict boundary.

3. Valvulogenesis

3.1 Endocardial Cushion Formation

During initial cardiac development, the primitive FHF-derived heart forms as a linear tube composed of only myocardium and an inner endocardial layer. The SHF provides additional endocardial cells (Verzi et al., 2005) during the looping process, including specialized cushion endocardial cells that will be activated and undergo EMT. These cells will ultimately be responsible for septating the common atria and ventricle as well as forming the cardiac valves.

Concurrent with the initiation of heart looping, extracellular matrix is secreted by the myocardial cells of the outflow tract (OFT) and the developing atrio-ventricular canal (AVC) (Krug et al., 1987). The secreted ECM, containing condroitin sulfate and hyaluronic acid, begins to occupy and expand within the regions between the myocardial and endocardial layers (Manasek, 1976). At E9.0 a specialized subset of endocardial cells adjacent to these accumulations of matrix, begin to undergo EMT. After receiving inductive signals from the myocardium and the surrounding ECM, cushion endocardial cells down-regulate genes associated with cell-to-cell adhesion, up-regulate mesenchymal markers, become hypertrophic, and invade the underlying ECM (cardiac jelly). By E10.5 a significant population of endocardial cells have undergone EMT and invaded the cardiac jelly residing at the OFT and AVC (PATTEN et al., 1948). This combination of mesenchymal cells and ECM proteins make up the structures known as the cardiac cushions. The cushion mesenchyme will proliferate and undergo remodeling into primitive valve structures that can be distinguished by E12.5.

The process of endocardial EMT is dependent on both cell-autonomous molecular cascades and cell non-autonomous signals from the surrounding cushion myocardium. *In vitro* invasion assays have shown the specificity of the interaction between myocardium underlying

the OFT and AVC and presumptive cushion endocardium. While myocardium isolated from the cushion regions is sufficient to induce EMT in cultured cushion endocardium, the same experiment performed with ventricular cardiomyocytes elicits no response from endocardial cells. Similarly, only the subset of endocardial cells surrounding the future cushions is competent to undergo activation and EMT (Runyan and Markwald, 1983; Mjaatvedt et al., 1987). The stringent requirement of this interaction results in EMT within the OFT and AVC without aberrant mesenchymal cells being induced within the cardiac chambers.

3.1 Role of the TGF-β Superfamily in EMT

The inductive capabilities of the cushion myocardium are conferred in part through the secretion of TGF-ß and BMP signaling ligands. Initial evidence implicating TGF-ß signaling in cushion development was performed in chick, where pan-TGF-ß blocking antibodies resulted in complete block in EMT within cushion endocardium *ex vivo* (Potts and Runyan, 1989). In the chick model, both TGF-ß2 and TGF-ß3 are required for EMT induction, while in mouse only TGF-ß2 is necessary (Camenisch et al., 2002). In the mouse model, TGF-ß2 expression is restricted to the OFT and AVC, and only expands after the completion of EMT at the cushions (Dickson et al., 1993). The functional necessity for TGF-ß2 has been illustrated with both *ex vivo* and *in vivo* loss-of-function experiments. Treatment of *ex vivo* cushion endocardium with TGF-ß2 blocking antibodies inhibits their activation (Camenisch et al., 2002). Genetic removal of TGF-ß2 *in vivo* results in a multitude of cardiac phenotypes including septal and outflow pathologies. However, EMT is only partially inhibited *in vivo*, highlighting the multiple layers of regulation within the developing cushions (Sanford et al., 1997).

Bone Morphogenetic Protein (BMP) signaling ligands are members of the TGF-β superfamily and also play a direct role in the induction of EMT within the cushion endocardium. During the embryonic window when EMT is being initiated within the endocardium, BMP-2, BMP-4, BMP-5, BMP-6 and BMP-7 are expressed in the OFT and AVC (Lyons et al., 1990). Similar to early studies with TGF-β, investigation into the role of BMPs in cushion EMT circumvented early embryonic lethality by using *ex vivo* culturing of AVC and OFT explants. Treatment of cushion endocardial explants with BMP-2 is sufficient to induce EMT with or without co-culture with cushion myocardium. This treatment also resulted in increased expression of TGF-ß, demonstrating crosstalk between TGF-ß superfamily members within the endocardium (Sugi et al., 2004). Analysis of multiple models of cardiac specific BMP4 loss-of-function suggests that BMP4 is not required for the initiation of EMT within the cushion endocardium. However, this BMP isoform plays a critical role in valve development, downstream of EMT, specifically by promoting cell proliferation within the cardiac cushions (Jiao et al., 2003; McCulley et al., 2008) . Single knockouts of BMP-5, BMP-6 or BMP-7 do not elicit cardiac defects (Dudley and Robertson, 1997). However, compound knockouts consisting of BMP-5/BMP-7 (Solloway and Robertson, 1999) and BMP-6/BMP-7 (Kim et al., 2001) fail to form cardiac cushions and exhibit delayed formation of OFT cushions respectively.

Chapter 4 will address intracellular regulation of TGF-ß and BMP signal transduction within the cushion endocardium. Specifically, novel requirements for the signal inhibiting molecules Smad6 and Smad7 during embryogenesis will be described.

4. Experimental Focus

While the majority of the mature heart is comprised of beating myocardium, non-cardiac structures composed of endothelial cells, smooth muscle and mesenchyme play important roles in the functionality of the organ. These include great vessel-heart interfaces, endocardium, coronary vasculature and valves. Compared to other fields, cardiac development research suffers from a relative paucity of specific molecular markers for the different sub-populations of cardiac progenitors and the diverse tissues derived from them. This can results in a lack of studies addressing the development of small, but critical portions of the mature heart, the majority of which are derived from SHF-progenitor cells.

In this dissertation we examine the regulation and development of diverse SHF fates within the embryonic heart. Specifically, we focus on the development of aortic smooth muscle and the cardiac valves. Our findings should further the knowledge of what regulates formation of these structures and highlight their development within the context of the cellular populations surrounding them.

CHAPTER TWO:

Nkx2-5 Lineage Tracing Visualizes the Distribution of Second Heart Field-derived Aortic Smooth muscle

genesis 51:862–869 (2013)

LETTER

Nkx2-5 Lineage Tracing Visualizes the Distribution of Second Heart Field-derived Aortic Smooth Muscle

Andrew W. Harmon,[1,2] **and Atsushi Nakano**[1,2,3,4]*

[1]Department of Molecular Cell and Developmental Biology, University of California, Los Angeles, Los Angeles, California

[2]Molecular Biology Institute, University of California, Los Angeles, Los Angeles, California

[3]Eli and Edythe Broad Center of Regenerative Medicine and Stem Cell Research, University of California, Los Angeles, Los Angeles, California

[4]Jonsson Comprehensive Cancer Center, University of California, Los Angeles, Los Angeles, California

Received 16 August 2013; Revised 10 October 2013; Accepted 11 October 2013

During embryogenesis, aortic smooth muscle originates from four major developmental sources: cardiac mesoderm, neural crest, somatic mesoderm, and splanchnic mesoderm (Majesky, 2007). It has been hypothesized that boundaries between smooth muscle from distinct embryonic origins represent areas of particular vulnerability to aortic dissection (Cheung *et al.*, 2012; Majesky *et al.*, 2011; Waldo *et al.*, 2005). Within the ascending aorta, such a boundary occurs where second heart field (SHF)-derived smooth muscle (Waldo *et al.*, 2005) meets neural crest cell (NCC)-derived smooth muscle (Jiang *et al.*, 2000; Le Lièvre and Le Douarin, 1975) at the base of the aorta.

Studies with markers for committed cardiac progenitors including Mef2c, Nkx2-5, FGF10, and Isl1 have traced the contribution of the SHF to aortic smooth muscle, however, the majority of these studies do not visualize the anatomical border between SHF- and NCC-derived smooth muscle within the ascending aorta. Mef2c-AHF-Cre and Nkx2-5-Cre are established markers of the SHF. However, previous aortic fate-mapping investigations with these lineages do not show the distribution of SHF-derived aortic smooth muscle with significant anatomic detail (Ma *et al.*, 2008; Verzi *et al.*, 2005). The results of these studies do not resolve the boundaries of SHF-derived cells with those of the NCC or within the specific layers of the aorta. Isl1-Cre has shown the distribution of SHF-derived aortic smooth muscle in more detail (Sun *et al.*, 2007), however, studies with this marker are complicated by the expression of Isl1 in a subset of NCCs, which results in the labeling of both mesoderm and ectoderm-derived smooth muscle at the base of the aorta (Engleka *et al.*, 2012).

To date the most detailed visualization of the boundary between SHF and NCC-derived smooth muscle has been with Mesp1-Cre (Choudhary *et al.*, 2009). Mesp1 is transiently expressed in the pre-cardiac mesoderm during early gastrulation (Saga *et al.*, 1999). Mesp1-Cre-derived smooth muscle is visible on the adventitial side of the aorta within the same region that Wnt1-labeled NCC-derived smooth muscle appears on the luminal side of the ascending aorta. However, this complimentary, but distinct, smooth muscle pattern has not been visualized using a committed cardiac progenitor lineage and the initiation of the smooth muscle boundary at the aortic base has not been directly observed.

Here we use Nkx2-5-Cre to provide the first detailed genetic tracing of the anatomic distribution of SHF-derived smooth muscle using a committed cardiac progenitor lineage. Using specific markers for the smooth muscle compartment and different developmental time points, we highlight the distinct anatomical distribution of SHF-derived cells as they recede to the adventitial

* Correspondence to: Atsushi Nakano, 615 Charles E. Young Dr. South, Los Angeles, CA 90095.
E-mail: anakano@ucla.edu

Contract grant sponsor: BSCRC; AHA; Contract grant number: GRNT9420039; Contract grant sponsor: NIH/NHLBI; Contract grant number: R21HL109938; Contract grant sponsor: National Institutes of Health; Contract grant number: T32 GM007185
Published online 4 November 2013 in
Wiley Online Library (wileyonlinelibrary.com).
DOI: 10.1002/dvg.22721

side of the media layer creating a vertical boundary with NCC-derived tissue in the ascending aorta and pulmonary trunk.

RESULTS

Distribution of SHF-Derived Outflow Tract Smooth Muscle During Embryogenesis

To determine the anatomical distribution of SHF derived smooth muscle in the embryonic outflow tract, lineage tracing was performed using *Nkx2-5-Cre* knockin mice (*Nkx2-5*$^{Cre/+}$) (Moses *et al.*, 2001) bred with *Rosa26-YFP* reporter mice (*R26*$^{YFP/YFP}$). The smooth muscle marker smMHC is not robustly expressed before E15.5, while early markers such as smooth muscle actin (SMA) and sm22α are additionally expressed in immature cardiomyocytes and the endocardial cushions. Therefore, we used two markers to differentiate between these cell types, scoring sm22α$^+$/cTnT$^+$ cells as immature cardiomyocytes and sm22α$^+$/cTnT$^-$ cells within the developing aorta and pulmonary trunk as embryonic smooth muscle.

First, lineage tracing was conducted prior to outflow tract septation at E10.5 (Fig. 1A). While the Nkx2-5 lineage labeled endothelial cells within both the outflow tract and the aortic sac (arrowheads), there were minimal YFP$^+$/sm22α$^+$/cTnT$^-$ cells surrounding the aortic sac (arrow). Analysis of the post-septation outflow tract at E12.5 showed that Nkx2-5-Cre visualizes primordial SHF-derived smooth muscle in the aorta and pulmonary trunk, which comprises the majority of smooth muscle proximal to the heart (Fig. 1B). Costaining with cTnT distinguishes the myocardial wall from the outflow media. Additionally, we analyzed transverse sections through the developing E12.5 aorta and pulmonary trunk (Fig. 1C,D). At the base of the aorta (1C, bottom) and pulmonary trunk (1D, bottom) extensive YFP expression is seen in the sm22α$^+$/cTnT$^-$ smooth muscle layer. Midway to the aortic root and arch (Fig. 1C, middle) as well as where the pulmonary trunk branches to the lungs (Fig. 1D, middle) YFP is expressed in a significant amount of smooth muscle, but markedly absent from the luminal side of the medial layer. Finally, within the distal ascending aorta (Fig. 1C, top) and the ductus arteriosus (Fig. 1D, top) YFP was absent from the medial layer. We observed YFP$^+$ endothelial cells within the aorta and pulmonary trunk throughout the transverse levels we examined (1C and 1D, arrowheads). These data show that the unique pattern of SHF-derived smooth muscle receding to the adventitial side of the media, previously described in adult tissue (Choudhary *et al.*, 2009), is established by E12.5 and persists throughout embryonic development.

The Nkx2-5-Cre Lineage Visualizes the Boundary Between SHF and NCC-Derived Smooth Muscle in the Post-Natal Aorta

Sections of neonatal *Nkx2-5*$^{Cre/+}$; *R26R*$^{YFP/+}$ hearts were stained with the mature smooth muscle-specific contractile protein smooth muscle myosin heavy chain (smMHC) and counterstained for YFP. Similarly to what was observed embryonically, YFP$^+$ cells constituted the majority of the smooth muscle compartment at the base of the aorta proximal to the heart (Fig. 2A, bracket) and then becomes restricted to the adventitial side of the media before becoming absent within the ascending aorta. YFP expression was also seen in the majority of endothelial cells of the aortic intima (arrow) and covering the aortic valve. In addition to labeling the majority of ventricular cardiomyocytes, our results showed YFP expression in the adventitia as well as a subset of valve mesenchyme (arrowhead), which originates from labeled cushion endocardium (Ma *et al.*, 2008; Nakano *et al.*, 2013).

For comparison, we conducted lineage tracing using *Wnt1-Cre* transgenic mice (Danielian *et al.*, 1998) to mark the neural crest lineage. Consistent with previous reports (Jiang *et al.*, 2000), *Wnt1-Cre*, *R26R*$^{YFP/+}$ lineage tracing shows the majority of the smooth muscle layer within the ascending aorta is YFP$^+$ (Fig. 2B, bracket). YFP expression is also present on the luminal side of the aortic media within the same region where Nkx2-5-Cre$^+$ SHF-derived smooth muscle is restricted to the adventitial side. This suggests a complimentary distribution of cells from these lineages within the media, that when combined, constitutes the entirety of smooth muscle in the ascending aortic. Committed cardiomyocyte lineages such as Myosin Light Chain 2v (Mlc2v)-Cre showed a complete lack of YFP expression in both smooth muscle and endothelial compartments (Fig. 2C).

To look in greater detail at the ability of the Nkx2-5 lineage to label the complimentary distribution of SHF and neural crest-derived aortic smooth muscle, transverse aortic sections of neonatal *Nkx2-5*$^{Cre/+}$, *R26*$^{YFP/+}$ animals were stained for YFP and the smooth muscle marker sm22α (Fig. 3A, solid lines). Representative transverse sections were analyzed at distances from the aortic annulus >500 μm (Fig. 3B), between 200 and 500 μm (Fig. 3C) and within 200 μm (Fig. 3D) and quantified for YFP expression within the smooth muscle layer (Fig. 3E). Taken together with Figure 2A, these data show in detail that while SHF and NCC-derived smooth muscle occupy distinct regions of the aortic media, they form a complimentary vertical boundary within the ascending aorta.

Nkx2-5-Cre Visualizes Coronary Artery Smooth Muscle

In addition to examining the outflow tracts, we examined Nkx2-5-Cre labeling in epicardially derived (Mikawa and Gourdie, 1996; Pérez-Pomares *et al.*, 2002) coronary smooth muscle. Analysis of *Nkx2-5*$^{Cre/+}$; *Rosa26*$^{YFP/+}$ neonatal sections showed YFP expression in a mosaic

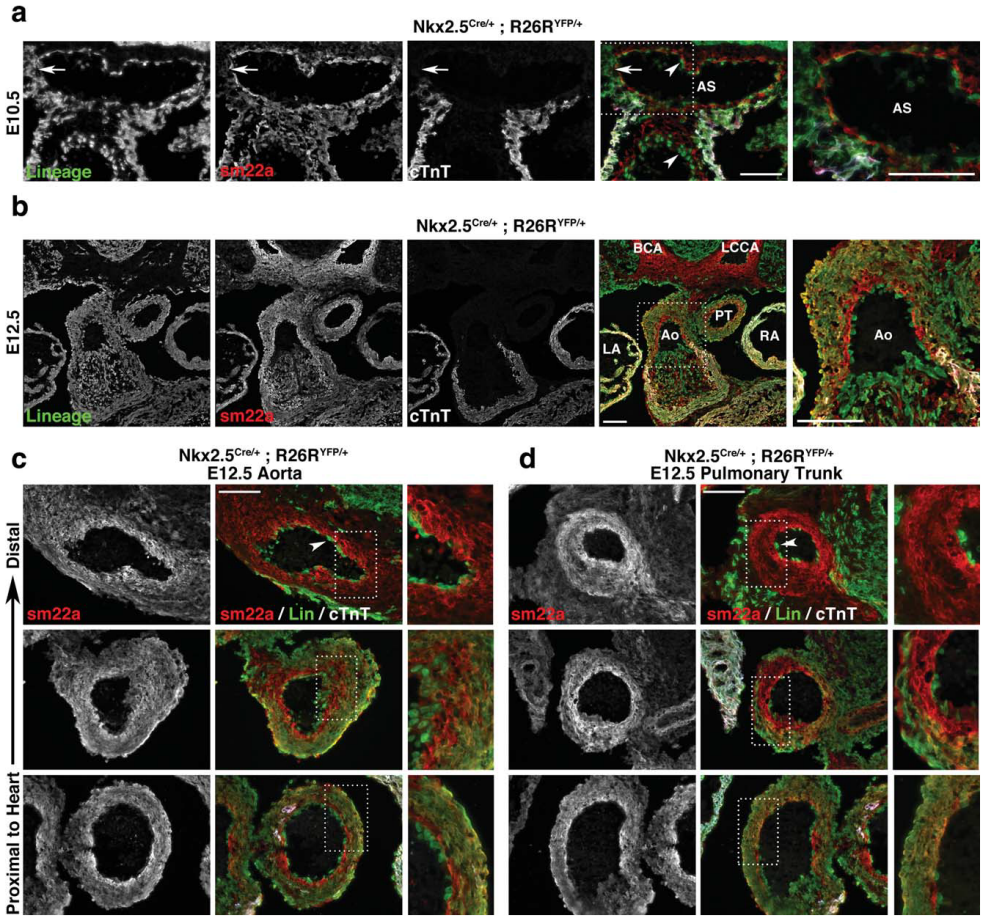

FIG. 1. Distribution of SHF-derived smooth muscle in the embryonic outflow tracts. Frontal and transverse sections of E10.5 and E12.5 *Nkx*2-5$^{Cre/+}$; *Rosa*26$^{YFP/+}$ embryos were stained for YFP (green), sm22α (red) and cTnT (white). Sm22α$^+$/cTnT$^-$ cells within the embryonic media were scored as developing smooth muscle, while Sm22α$^+$/cTnT$^+$ cells represented immature cardiomyocytes. (**A**) At E10.5, few YFP$^+$/sm22α$^+$/cTnT$^+$ cells are seen surrounding the aortic sac (arrow), while a significant number of YFP$^+$ endothelial cells are present in the developing outflow tract and aortic sac (arrowheads). (**B**) At E12.5, YFP$^+$/sm22α$^+$/cTnT$^-$ smooth muscle cells are visible within the majority of the developing media and intima of the aorta and pulmonary trunk. (**C, D**) Staining of transverse sections of the aorta and pulmonary trunk. YFP$^+$ smooth muscle is present throughout the smooth muscle layer within the aorta and pulmonary trunk proximal to the heart (bottom). Further from the heart YFP expression recedes to the adventitial side of the vessel (middle) before becoming absent (top). YFP+ endothelial cells are seen throughout each transverse section, including distal sections (top, arrowheads). Ao—aorta; AS—aortic sac; BCA—brachiocephalic artery; LA—left atrium; LCCA—left common carotid artery; PT—pulmonary trunk; RA—right atrium. Scale bars equal 100 μm.

pattern throughout the smooth muscle layer of the main coronary arteries (Fig. 4, top, arrowheads) and small coronary branches (Fig. 4, arrows). In addition, YFP was observed in a significant number of coronary endothelial cells. These results showed similar efficiency in visualizing Nkx2-5-Cre labeled coronary smooth muscle and endothelial cells as previous approaches (Ma *et al.*, 2008), but without the necessity of a specialized reporter allele. Nkx2-5-Cre labeling was additionally compared to the neural crest lineage, which also contributes to coronary smooth muscle proximal to the aorta. As previously described

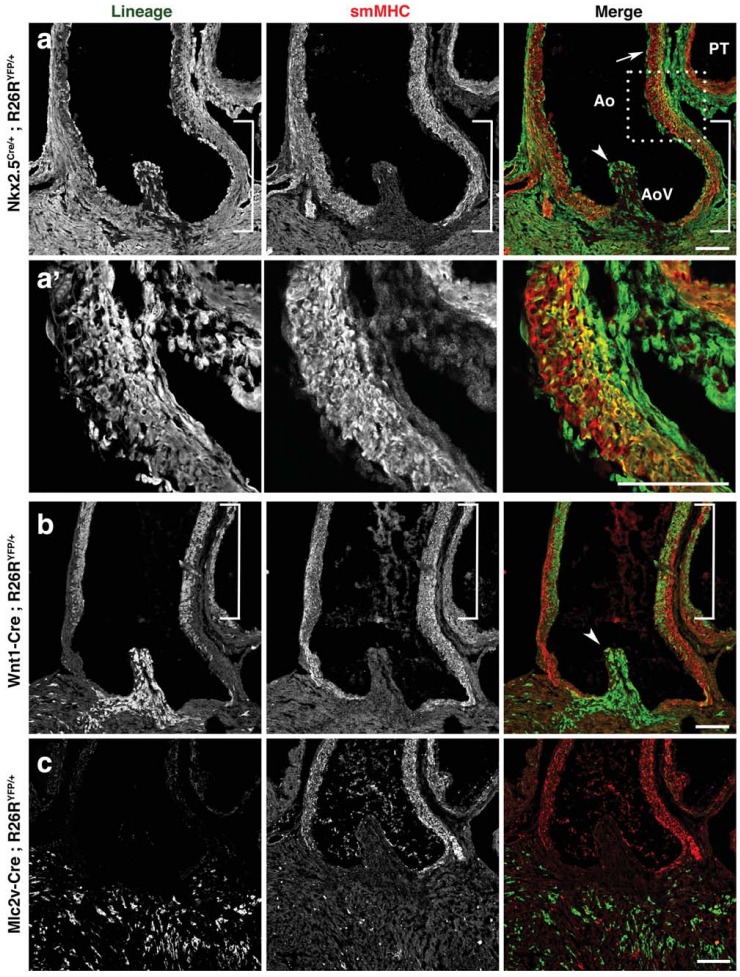

FIG. 2. Distribution of Nkx2-5-Cre^{+} SHF-derived smooth muscle in the post-natal aorta. Lineage labeling was performed using *Nkx2-5-*, *Wnt1-* and *Mlc2v-Cre* lines crossed to a *Rosa26*$^{YFP/YFP}$ reporter line. Frontal sections of P0 neonatal hearts were stained for YFP (green) and the smooth muscle compartment (smMHC, Red). (**A**) The Nkx2-5-Cre labeled SHF lineage contributes substantially to smooth muscle at the base of the aorta (bracket). (A, **A'**) YFP expression recedes to the adventitial side of the media and becomes absent before the aortic arch. YFP^{+} cells are observed within the intima (arrow), aortic valve mesenchyme (arrowhead) and the endothelial lining of the aortic valve. (**B**) The Wnt1-Cre labeled neural crest lineage comprises the majority of valve mesenchyme (arrowhead) and is present on the luminal side of the media before constituting the majority of smooth muscle within the ascending aorta (bracket). (**C**) Lineage analysis using the committed cardiac lineage *Mlc2v-Cre* did not result in the labeling of aortic smooth muscle or endothelial cells. Ao—aorta; PT—pulmonary trunk; AoV—aortic valve. Scale bars equal 100 μm.

(Jiang *et al.*, 2000), NCC contribution is reduced within the descending coronary vessels and absent distal to the aorta (Fig. 4, bottom). Of note, *Wnt1-Cre*; *Rosa26*$^{YFP/+}$ neonatal heart sections show mosaic YFP expression in the smooth muscle of the proximal coronary arteries, indicating that smooth muscle cells of this region are not exclusively derived from NCCs. The presence of Nkx2-5 and Wnt1-derived smooth muscle within the same region suggest that proximal to the aorta, coronary smooth muscle from different

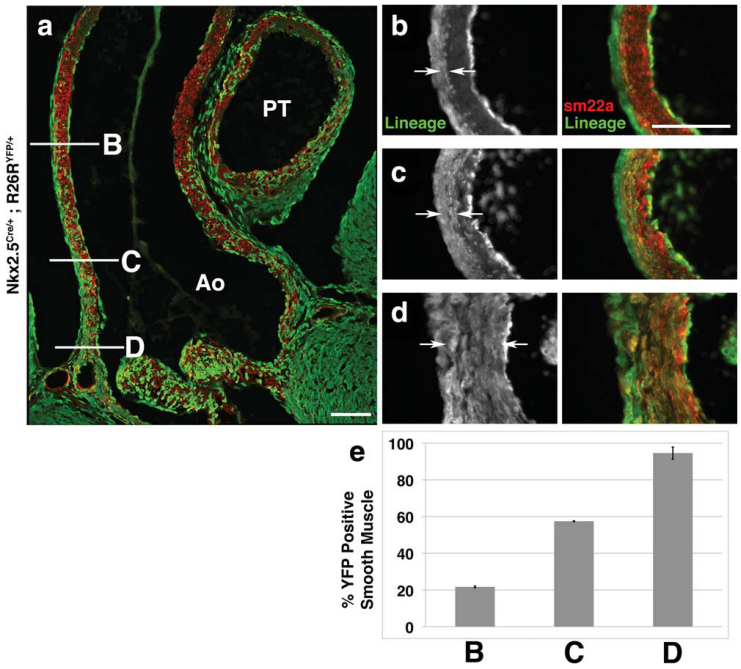

FIG. 3. Nkx2-5 visualizes the boundary between SHF and neural crest-derived smooth muscle in the ascending aorta. Sections of P0 neonatal *Nkx2-5*$^{Cre/+}$; *Rosa26*$^{YFP/+}$ aortae were analyzed at representative distances from the aortic annulus. (**A**) Frontal section of the aorta stained for YFP (green) and the smooth muscle marker sm22α (red). Solid lines denote the level and plane of stained transverse sections in B–D. (**B–D**) Transverse aortic sections from *Nkx2-5*$^{Cre/+}$; *Rosa26*$^{YFP/+}$ neonates. (B) At 540 μm distal from the aortic annulus, the majority of the smooth muscle does not express YFP. (C) At 295 μm from the annulus more than half of aortic smooth muscle is YFP$^+$, but this expression is restricted to the adventitial side of the smooth muscle layer. (D) A transverse section at the base of the aorta, 86 μm from the annulus, shows nearly the entire smooth muscle is YFP$^+$. (**E**) Quantification of Nkx2-5$^+$ progenitor contribution to aortic smooth muscle at representative transverse levels, excluding signal within the intima and adventitia. Error bars represent the standard deviation of three measurements. Scale bars equal 100 μm.

origins do not reside in mutually exclusive regions and do not form a clear boundary like within the aorta.

DISCUSSION

Previous fate mapping studies using *Nkx2-5-Cre* knockin lines have reported limitations with standard *Rosa26-LacZ* reporter alleles, showing labeling that is restricted to a cardiomyocyte fate (Ma *et al.*, 2008). Here we demonstrate sufficient sensitivity using the *Rosa26-YFP* reporter and antibody based fluorescent detection to visualize Nkx2-5-derived smooth muscle and endothelial cells in addition to cardiomyocytes.

Several studies have highlighted lineage-specific responses to extracellular stimuli from smooth muscle from different developmental origins (Cheung *et al.*, 2012; Gadson *et al.*, 1997; Topouzis and Majesky, 1996). These findings raise the hypothesis that an incoherent response from two different groups of adjacent smooth muscle may underlie pathologies associated with the aortic media such as dissection. As the creation of a false lumen during aortic dissection can involve splitting of the medial layer (Macura *et al.*, 2003), a potential mechanism for the propagation of type 1 and type 2 dissection could be along the vertical seam between SHF and neural crest-derived smooth muscle (Fig. 5).

One obstacle of directly testing these hypotheses is that aortic smooth muscle from different embryonic origins is histologically indistinguishable, requiring lineage based labeling to visualize smooth muscle borders. We use Nkx2-5-Cre lineage tracing to build on previous aortic fate-mapping studies, showing the distribution of SHF-derived smooth muscle within the embryonic and

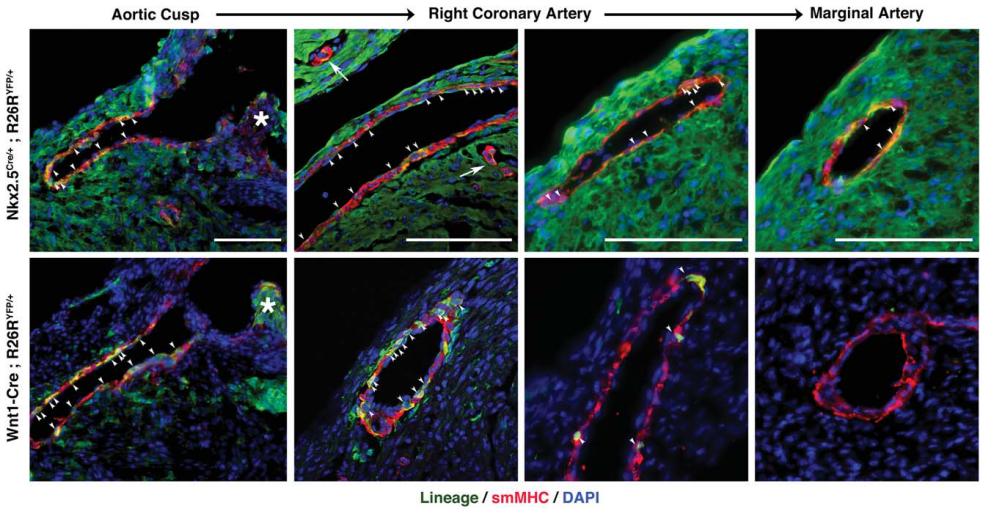

FIG. 4. Nkx2-5-Cre lineage tracing in the coronary arteries. Frontal sections of P0 neonatal Nkx2-5$^{Cre/+}$; Rosa26$^{YFP/+}$ and Wnt1-Cre; Rosa26$^{YFP/+}$ hearts were stained for YFP (green), smMHC (red) and DAPI (blue). (Top) Nkx2-5-Cre labels a significant, but incomplete, portion of the coronary artery's smooth muscle layer (arrowheads). Mosaic YFP expression is observed throughout the smooth muscle of the main right coronary artery from the arotic cusp (left) to within the right marginal artery (right), as well as in small coronary branches (arrows). YFP$^+$ endothelial cells can also be observed luminal to the marked smooth muscle compartment. (Bottom) Lineage tracing using Wnt1-Cre labels a significant subset, but not all, of smooth muscle (arrowheads) within the coronary artery proximal to the aortic cusp (left two panels). YFP expression is limited within the main coronary artery (third panel) and is absent within the right marginal artery distal to the aorta (right). *—aortic valve, scale bars equal 100 μm.

post-natal outflow tracts becomes restricted to the adventitial side forming a complimentary boundary with neural crest-derived smooth muscle. Use of a widely available cardiac progenitor lineage marker, such as Nkx2-5-Cre, within the genetic background of models of aortic dissection could be one approach for mapping dissection initiation in regards to the border of SHF-derived aortic smooth muscle.

EXPERIMENTAL PROCEDURES

Mice and Animal Husbandry

This investigation conforms to the Guide for the Care and Use of Laboratory Animals published by the US National Institute of Health (NIH Publication No. 85-23, revised 1996). All animal protocols, experiments, and housing were performed following Institutional Approval for Appropriate Care and use of Laboratory animals by the UCLA Institutional Animal Care and Use Committee (Chancellor's Animal Research Committee (ARC)), Animal Welfare assurance number A3196-01.

Cardiac and neural crest cell specific Cre recombinase lines were crossed to *Rosa26*$^{YFP/YFP}$ females as follows. The neural crest cell lineage was traced with using mice containing Cre under the control of Wnt1 enhancer elements (*Wnt1-Cre*, *Rosa26*$^{YFP/+}$) (Danielian *et al.*, 1998). The common cardiac/common second heart field progenitor lineage was traced with Cre knocked into one allele of the Nkx2-5 locus (*Nkx2-5*$^{Cre/+}$, *Rosa26*$^{YFP/+}$) (Moses *et al.*, 2001). First heart field and anterior heart field derived cardiomyocytes were traced with Cre under the control of Mlc2v promoter elements (*Mlc2v-Cre*, *Rosa26*$^{YFP/+}$) (Chen *et al.*, 1998). Noon of the day a vaginal plug was detected was considered embryonic day (E) 0.5. The day when newly born pups were discovered was considered postnatal day (P) 0.

Histology and Immunostaining

Embryonic dissections were performed in phosphate buffered saline supplemented with 1 mM EDTA. The pericardial wall was removed and embryos E12.5 or older were beheaded before fixation. Embryos were fixed on ice in 4% paraformaldehyde for 1–2 h depending on age. After washing, embryos were cryoprotected in 30% sucrose/PBS overnight. Embryos were transferred to a 1:1 mixture of 30% sucrose/PBS and OCT (Sakura, Torrance, CA) for 2 h and then incubated in OCT for 1 h and frozen in a bath of isopropanol and dry ice. Perinatal hearts were perfused with 4% PFA and

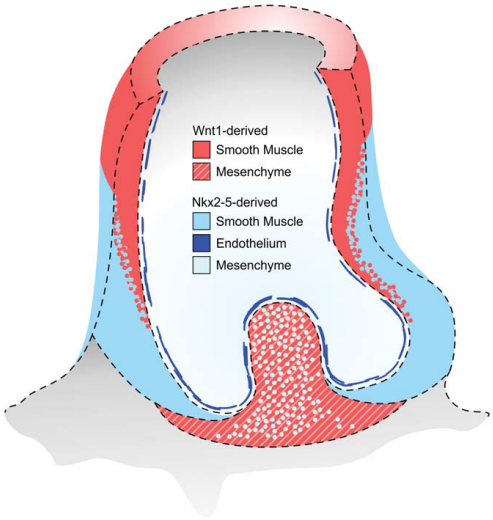

FIG. 5. Model of the second heart field-neural crest smooth muscle boundary. Smooth muscle at the base of the aorta is derived from SHF progenitors. The SHF contribution to the media then forms a vertical seam complimentary with neural crest-derived smooth muscle before being replaced entirely within the ascending aorta. SHF-derived endothelial cells constitute the majority of the aortic intima within the base of the aorta and a portion of the ascending aorta, including the endothelial layer of the aortic valve. While the majority of aortic valve mesenchyme is derived from the neural crest, a subset of cells within this region come from a cardiac progenitor source.

removed with the assistance of a pin board. Embedding was then carried out similarly to embryonic dissections.

Immunofluorescent stainings were performed as follows: 8–10 μm fixed frozen sections were blocked with 10% normal goat serum; 0.1% TritonX. Antibody reactions were carried out in 5% normal goat serum for 1 h at room temperature or at 4°C overnight. Fluorescent conjugated secondary antibody reactions were performed in 5% normal goat serum for 1 h at room temperature. Slides were mounted with ProLong Gold DAPI media (Invitrogen). Alternatively, when primary antibodies raised in mice were used, staining was performed using M.O.M. reagents (Vector Labs) as described in the manufacturer's protocol.

Antibodies used and their working concentrations are as follows: mouse anti-cTnT (1:200, Lab Vision, Fremont, CA), rabbit anti-smMHC (1:200, Biomedical Technologies, Stoughton, MA), rabbit anti-sm22α (1:200, Abcam, Cambridge, UK), chicken anti-GFP (1:1000, Aves Labs, Tigard, OR). For immunofluorescent detection the following Alexafluor conjugated secondary antibodies were used: goat anti-mouse-647, goat anti-chicken-488, goat anti-rabbit-594 (1:1000, Invitrogen, Grand Island, NY).

Image Analysis

Immunofluorescent imaging was performed on a Zeiss AxioImager system using Axiovision release 4.8. Confocal microscopy was performed on a Zeiss Laser Scanning Microscope (LSM) 780 system using the 2010 release of Zen image acquisition software.

ACKNOWLEDGMENTS

The authors thank the UCLA Broad Stem Cell Research Center for the use of their confocal microscope, Donna Crandall for the digital illustration of Figure 5 and Matthew Veldman, Xiaoqian Liu and Katrina Adams for feedback on the manuscript.

LITERATURE CITED

Chen J, Kubalak SW, Chien KR. 1998. Ventricular muscle-restricted targeting of the RXRalpha gene reveals a non-cell-autonomous requirement in cardiac chamber morphogenesis. Development 125: 1943–1949.

Cheung C, Bernardo AS, Trotter MWB, Pedersen RA, Sinha S. 2012. Generation of human vascular smooth muscle subtypes provides insight into embryological origin-dependent disease susceptibility. Nat Biotechnol 30:165–173.

Choudhary B, Zhou J, Li P, Thomas S, Kaartinen V, Sucov HM. 2009. Absence of TGFbeta signaling in embryonic vascular smooth muscle leads to reduced lysyl oxidase expression, impaired elastogenesis, and aneurysm. Genesis 47:115–121.

Danielian PS, Muccino D, Rowitch DH, Michael SK, McMahon AP. 1998. Modification of gene activity in mouse embryos in utero by a tamoxifen-inducible form of Cre recombinase. Curr Biol 8:1323–1326.

Engleka KA, Manderfield LJ, Brust RD, Li L, Cohen A, Dymecki SM, Epstein JA. 2012. Islet1 derivatives in the heart are of both neural crest and second heart field origin. Circ Res 110:922–926.

Gadson PF, Dalton ML, Patterson E, Svoboda DD, Hutchinson L, Schram D, Rosenquist TH. 1997. Differential response of mesoderm- and neural crest-derived smooth muscle to TGF-beta1: regulation of c-myb and alpha1 (I) procollagen genes. Exp Cell Res 230:169–180.

Jiang X, Rowitch DH, Soriano P, McMahon AP, Sucov HM. 2000. Fate of the mammalian cardiac neural crest. Development 127:1607–1616.

Le Lièvre CS, Le Douarin NM. 1975. Mesenchymal derivatives of the neural crest: analysis of chimaeric quail and chick embryos. J Embryol Exp Morphol 34: 125–154.

Ma Q, Zhou B, Pu WT. 2008. Reassessment of Isl1 and Nkx2-5 cardiac fate maps using a Gata4-based reporter of Cre activity. Dev Biol 323:98–104.

Macura KJ, Corl FM, Fishman EK, Bluemke DA. 2003. Pathogenesis in acute aortic syndromes: Aortic dissection, intramural hematoma, and penetrating atherosclerotic aortic ulcer. Am J Roentgenol 181:309–316.

Majesky MW. 2007. Developmental basis of vascular smooth muscle diversity. Arterioscler Thromb Vasc Biol 27:1248–1258.

Majesky MW, Dong XR, Hoglund VJ. 2011. Parsing aortic aneurysms: more surprises. Circ Res 108:528–530.

Mikawa T, Gourdie RG. 1996. Pericardial mesoderm generates a population of coronary smooth muscle cells migrating into the heart along with ingrowth of the epicardial organ. Dev Biol 174:221–232.

Moses KA, DeMayo F, Braun RM, Reecy JL, Schwartz RJ. 2001. Embryonic expression of an Nkx2-5/Cre gene using ROSA26 reporter mice. Genesis 31:176–180.

Nakano H, Liu X, Arshi A, Nakashima Y, van Handel B, Sasidharan R, Harmon AW, Shin J-H, Schwartz RJ, Conway SJ, Harvey RP, Pashmforoush M, Mikkola HKA, Nakano A. 2013. Haemogenic endocardium contributes to transient definitive haematopoiesis. Nat Commun 4:1564.

Pérez-Pomares JM, Carmona R, González-Iriarte M, Atencia G, Wessels A, Muñoz-Chápuli R. 2002. Origin of coronary endothelial cells from epicardial mesothelium in avian embryos. Int J Dev Biol 46: 1005–1013.

Saga Y, Miyagawa-Tomita S, Takagi A, Kitajima S, Miyazaki JI, Inoue T. 1999. MesP1 is expressed in the heart precursor cells and required for the formation of a single heart tube. Development 126:3437–3447.

Sun Y, Liang X, Najafi N, Cass M, Lin L, Cai C-L, Chen J, Evans SM. 2007. Islet 1 is expressed in distinct cardiovascular lineages, including pacemaker and coronary vascular cells. Dev Biol 304:286–296.

Topouzis S, Majesky MW. 1996. Smooth muscle lineage diversity in the chick embryo. Two types of aortic smooth muscle cell differ in growth and receptor-mediated transcriptional responses to transforming growth factor-beta. Dev Biol 178:430–445.

Verzi MP, McCulley DJ, De Val S, Dodou E, Black BL. 2005. The right ventricle, outflow tract, and ventricular septum comprise a restricted expression domain within the secondary/anterior heart field. Dev Biol 287:134–145.

Waldo KL, Hutson MR, Ward CC, Zdanowicz M, Stadt HA, Kumiski D, Abu-Issa R, Kirby ML. 2005. Secondary heart field contributes myocardium and smooth muscle to the arterial pole of the developing heart. Dev Biol 281:78–90.

CHAPTER THREE:

The Role of Myocardin in cardiogenesis and the Development of SHF-derived Smooth Muscle

Introduction

During cardiogenesis common cardiac progenitors, marked by Flk1/Isl1/Nkx2-5, display multipotency and give rise to the three lineages that comprise the functional heart: cardiac muscle, smooth muscle and endothelial cells (Kattman et al., 2006; Moretti et al., 2006; Wu et al., 2006). While it has been suggested that these progenitors lose their ability to differentiate into endothelial cells early during heart development, the cardiac and smooth muscle lineages stay closely related until later in cardiogenesis (Wu et al., 2006; Nakano et al., 2011). The cardiac chambers do not contain a medial layer like the vessels they feed into, but cardiac progenitor-derived smooth muscle is essential for the proper development of the out-flow tracts (Waldo et al., 2005) as well as the coronary vasculature (Mikawa and Gourdie, 1996).

While the majority of aorta and pulmonary trunk arise from developmental origins distinct from the primordial heart tube, they must establish anatomical and functional continuity with the heart early in development. The importance of cardiac progenitor multipotency is highlighted at these boundaries, as beating striated cardiac muscle must transition to non-striated vascular smooth muscle while withstanding the hemodynamic stress of circulating blood. It has been suggested that abnormalities within this process can be the underlying cause of congenital heart malformations eventually leading to major cardiovascular diseases such as aortic dissection aneurysm and atrial fibrillation (Waldo et al., 2005; Majesky, 2007; Harmon, and Nakano, 2013).

The Serum Response Factor (SRF) transcription factor is a key regulator of cell growth as well as the differentiation of smooth, cardiac and skeletal muscle. SRF directs gene expression by binding conserved cis regulatory serum response elements, also known as CArG box motifs, which are present within the promoter elements of muscle specific genes (Norman et al., 1988).

While SRF is almost ubiquitously expressed, it gains DNA binding specificity through several mechanisms including interactions with a series of tissue specific co-factors (Miano, 2003). Among these is the cardiac and smooth muscle specific Myocardin (Myocd) (Du et al., 2003). Myocd directly interacts with SRF, promoting the transcription factor's localization to gene promoter elements (Wang et al., 2003). Global *Myocd* knockout animals exhibit complete loss of vascular smooth muscle development and are embryonic lethal at embryonic day 10.5 (E10.5) (Li et al., 2003).

While initially implicated in vascular smooth muscle development, studies using embryonic stem cell chimeric analysis have eloquently shown a strict requirement for *Myocd* for development of ventricular cardiomyocytes and visceral smooth muscle (Hoofnagle et al., 2011). Interestingly only a marginal requirement for *Myocd* was seen in vascular smooth muscle of the thoracic aorta in these studies. While this result differs from the complete loss of smooth muscle differentiation seen in global knockouts, there may be phenotypic variation based on assay or from functional compensation by Myocardin Related Transcription Factors (MRTFs) (Li et al., 2005). Cre/Lox studies have additionally shown that loss of *Myocd* within adult cardiomyocytes leads to fibrosis and heart failure (Huang et al., 2009). However, it is unknown whether the requirement for *Myocd* is uniform between atrial and ventricular cardiomyocytes and whether conditional knockout during development would translate into embryonic heart defects in addition to what has been observed in adults.

Within the ascending aorta, *Myocd* has been shown to be required for the proper differentiation of cardiac neural crest cells into smooth muscle (Huang et al., 2008). This is in contrast to what was observed within chimeric studies of the thoracic aorta, which is derived from somitic precursor cells (Hoofnagle et al., 2011). Within the ascending aorta ectodermally-

derived smooth muscle from the cardiac neural crest forms a histologically indistinguishable transition to mesodermally-derived smooth muscle from the SHF, yet whether *Myocd* is required within SHF-derived smooth muscle within the aorta has not been investigated.

Lack of *in vivo* studies of cardiac progenitor-derived smooth muscle may be due to unique challenges associated with the study of SHF-derived smooth muscle differentiation. Compared to other portions of the aorta, the SHF-derived aortic base represents a much smaller cell population. Sorting based strategies are also complicated due to cardiomyocytes making up the vast majority of SHF-lineage traced derivatives. These challenges also hold true in regards to studying smooth muscle within the vena cava (inflow tract), but to an even greater extent given that the inflow tract contains a myocardial sheath and only a minimal 1-2 cell layer thick smooth muscle layer. Additionally, a lack of genetic tools specific to the posterior second heart field has further hindered studies of in-flow smooth muscle.

In this study we use a recently described *Sarcolipin* (*Sln*)-Cre line (Nakano et al., 2011), specific to atrial progenitors derived from the SHF, to assess the role of *Myocd* within the atrial myocardium and inflow smooth muscle. Surprisingly, despite a reported requirement for *Myocd* within the adult myocardium (Huang et al., 2009), *Sln*-Cre conditional knockout animals exhibited no phenotype in regards to the development and survival of both cardiac and smooth muscle. We additionally used the common cardiac progenitor specific *Nkx2-5*-Cre knock-in line (Moses et al., 2001) to investigate the requirement of *Myocd* in developing cardiomyocytes as well as SHF-derived smooth muscle within the aorta and pulmonary trunk. Our developmental study confirms the role of *Myocd* in cardiomyocyte survival previously seen in adult cardiomyocytes, but does not observe smooth muscle defects within the SHF-derived aortic media. Our findings show that loss of *Myocd* during cardiogenesis leads to heart failure and

perinatal death, suggesting that there may be differential requirements for *Myocd* within cardiac progenitors based on their spatial and cellular fate within the mature heart.

Results

Myocardin is not necessary for development of atrial progenitors derived from the posterior second heart field

The sarcomeric gene *Sln* (MacLennan et al., 1985) is specifically expressed within atrial progenitors derived from the posterior SHF starting at E10.0. The recently described *Sln*-Cre line traces the fate of these progenitors to the myocardium of the atria and portions of the vena cava (Nakano et al., 2011). To examine the role Myocd plays within the development of these structures, we used this lineage in combination with a floxed *Myocd* allele (Huang et al., 2008). *Sln*-Cre; *Myocardin*$^{fl/fl}$ mutant animals did not exhibit defects in growth, survival or breeding viability compared to control littermates. Survivorship analysis shows that conditional mutants have life spans comparable to wildtype and heterozygote controls (Figure 3-1A). To determine if conditional knockout animals exhibited signs of cardiac stress despite normal survival rates, we looked at gross characteristics of adult hearts starting at six months of age (Figure 3-1C). When the ratio of heart weight over femur length is measured there is no significant difference between mutant and control animals (Figure 3-1B). Histological analysis also shows no defects within the cardiomyocytes of the atrial chambers or within the smooth muscle of the in-flow tract (not shown).

Myocardin is sufficient to drive posterior SHF-progenitors to a smooth muscle fate

To examine the ability of Myocd to direct the smooth the muscle differentiation of atrial progenitor cells, we developed an *ex vivo* co-culture system to label and maintain cells isolated from the *Sln*-Cre^{+} lineage. *Ex vivo* culture of S*ln*$^{+}$ progenitor cells was used in combination with an adenoviral vector that drives expression of *Myocd* under the control of cytomegalovirus

(CMV) promoter elements (Adv-*Myocd*). *Sln*-Cre; Rosa26$^{LacZ/+}$ hearts were isolated at E12.5, enzymatically dissociated and plated on an OP9 mesenchymal feeder layer.

Cultured *Sln*-Cre^{+} progenitors infected with Adv-*Myocd* contain a significantly higher population of lineage labeled cells expressing the mature smooth muscle marker Smooth Muscle Myosin Heavy Chain (smMHC), compared to progenitors infected with empty virus (Adv-*Control*) that show little or no spontaneous expression of smMHC (Figure 3-2A,B). This assay was also performed using progenitor cells from *Sln*-Cre; Rosa26$^{YFP/+}$ hearts. After infection, YFP^{+} atrial progenitors were purified from OP9 feeder cells via FACS and subjected to RNA isolation and semi-quantitative PCR. Similar to what is observed on the protein level, *Sln*-Cre^{+} progenitors infected with Adv-*Myocd* show increased mRNA expression of the smooth muscle markers *sm22a* and *smMHC* (Figure 3-2C). Taken together these data suggest that forced expression of *myocd* is sufficient to push atrial progenitors toward a smooth muscle fate.

Given the role Notch signaling plays in vascular smooth muscle development and its interaction with SRF (Morrow et al., 2008), we examined whether Notch plays a regulatory role in *Myocd*'s ability to induce smooth muscle differentiation in atrial progenitors *ex vivo*. We began by performing loss-of-function studies using the chemical Notch inhibitor DAPT. Using our *ex vivo* culturing system, *Sln*-Cre; Rosa26$^{YFP/+}$ progenitors cells were exposed to various concentrations of DAPT. We found that a 50uM concentration of DAPT significant inhibited expression of the Notch response gene *Hes1* without affecting cell viability (Figure 3-3A). Adv-*Myocd* infection plus DAPT treatment does not demonstrate a significant increase in smMHC gene transcription compared to Adv-*Myocd* infection alone. However, when cells were treated with empty virus, a modest increase in *smMHC* expression is observed in DAPT treated progenitors compared to DMSO only controls (Figure 3-3B). To further investigate a potential

role for Notch signaling in atrial progenitor differentiation and to eliminate the possibility that the strength of Adv-*Myocd* masks the effects of DAPT treatment, we moved to an *in vivo* Notch loss-of-function model.

To determine if Notch signaling is required *in vivo* for correct differentiation of atrial progenitor cells, we conditionally crossed *RPBjκ*$^{fl/fl}$ animals (Tanigaki et al., 2002) to the *Sln*-Cre line. Similarly to atrial specific knockout of *Myocd*, *Sln*-Cre; *RPBjκ*$^{fl/fl}$ animals are completely viable and show no defects in survival or cardiac development (not shown). Taken together, these experiments suggest that *Myocd* is sufficient to drive smooth muscle differentiation of atrial progenitor cells *ex vivo*, but a strict requirement for *Myocd* and canonical Notch signaling, in the development of atrial cardiomyocytes or in-flow smooth muscle, is not observed .

Myocardin is required for cardiomyocyte survival, but not SHF-derived smooth muscle differentiation

Previous studies using ES-cell chimerism have shown a requirement for *Myocd* within ventricular cardiomyocytes as well as within aortic smooth muscle (Hoofnagle et al., 2011). However, knockout studies of *Myocd* within the cardiac progenitor lineages making up these tissues have not been performed. To examine the role *Myocd* plays in cardiac development, we used *Nkx2-5*-Cre knock-in mice (*Nkx2-5*$^{Cre/+}$) (Moses et al., 2001). Nkx2-5 is a cardiac specific transcription factor that marks common cardiac progenitor cells and their derivatives within both the anterior and posterior second heart field. *Nkx2-5*-Cre efficiently marks the cardiomyocytes of each cardiac chamber as well as a subset of SHF-derived endocardial cells. Within the aorta

and pulmonary trunk *Nkx2-5*-Cre labels both SHF-derived endothelial and smooth muscle cells (Harmon, and Nakano, 2013).

Our results show that *Nkx2-5*$^{Cre/+}$; *Myocd*$^{fl/fl}$ animals are embryonic viable, but living mutants are not observed at the time of weaning. Examination of neonatal time points shows the majority of mutant animals die at postnatal day 2 (P2) with none observed after P12 (Figure 3-4). At P0 mutants appear modestly smaller than control littermates, but show no gross anatomical defects (Figure 3-5 A). PO mutant hearts are of comparable size to controls and appear normally developed, including the presence correctly organized outflow tracts (Figure 3-5 C,D). By P2 mutant animals are significantly smaller than littermates and exhibit less pigmentation (Figure 3-5B). Mutant hearts do not display significant differences in size at P2 compared to control, but had abnormal indentations and discoloration within the central portion of the ventricular myocardium (Figure 3-5 E-G).

Histological analysis shows that conditional mutants have phenotypically normal outflow tracts with vessel dilation and smooth muscle marker expression equivalent to controls (Figure 3-6). Analysis of the myocardium shows that the phenotype seen in whole mount is not superficial to the cardiac chambers, but is due to an extensive myocardial lesion within the left ventricle (Figure 3-7 A-D). Interestingly, Mason's Tri-Chrome staining of these lesions reveals aberrant collagen deposition, even though this phenomenon is more common later in postnatal diseases (Figure 3-7 C, D'). The presence of fibrotic tissue within the ventricular chambers is suggestive of muscle failure and cell death. Within the left ventricular chamber, distinct populations of enucleated (Figure 3-7 D, arrow) and nucleated (Figure 3-7 D, arrowhead) blood cells appear associated with the fibrotic lesion, spanning the entire length of the affected tissue. To determine the identity of these cells, histological sections of mutant hearts were stained with hematopoietic

surface markers. These results show that enucleated Ter119^{+} erythroid cells are preferentially found proximal to the affected ventricular septum (Figure 3-8 A). CD41^{+} platelets are found within the fibrotic muscle tissue (Figure 3-8 B), while an aggregation of CD45^{+} leukocytes several cell layers thick is present within directly luminal to the lesion (Figure 3-8 C). Taken together these results suggest that embryonic loss of *Myocd,* in *Nkx2-5*$^{+}$ cardiac progenitors, results in cardiac muscle failure shortly after birth, leading to fibrosis and eventually the acquisition of mural thrombi within the endocardial wall.

Discussion

Here we describe the role that the SRF co-factor *Myocd* plays in the differentiation and survival of cardiac and smooth muscle within the developing heart. We show that *Myocd* is dispensable for the development of atrial progenitor-derived cardiomyocytes and smooth muscle, but is essential for the survival and function of the ventricular myocardium. Evidence for *Myocd*-dependant cardiomyocyte differentiation and development has previously been shown with ESC-chimeric analysis (Hoofnagle et al., 2011), but this is in stark contrast to initial global *Myocd* knockout embryos, which exhibit no cardiac defects before dying at E10.5 (Li et al., 2003). Despite these discrepancies, a requirement for *Myocd* had not previously been tested genetically in cardiac progenitor lineages.

Conversely to the enlargement and fibrosis of all four cardiac chambers when *Myocd* is genetically removed in adult hearts (Huang et al., 2009), our study found a disparity in the need for *Myocd* between the ventricles and atria. Genetic excision with atrial progenitor specific *Sln*-Cre did not result in any myocardial defects and *Sln*-Cre myocd$^{fl/fl}$ animals remained unaffected and viable through adulthood. The other Cre recombinase lineage used in this study, knock-in *Nkx2-5*-Cre, results in the excision of *Myocd* from the developing cardiomyocytes of all four cardiac chambers. However, our study only observed fibrosis and cardiomyocyte failure in the ventricles. An interesting hypothesis is that the increased requirement for a survival factor such as *Myocd* in the ventricles compared to the atria may be directly correlated to the increased contractile force required from the former vs. the latter. Given that *Sln*-Cre *Myocd*$^{fl/fl}$ mutants did not show a phenotype, the atrial hypertrophy shown in adult knockout animals may be secondary to muscle failure within the ventricle. This agrees with previous ES-cell analysis that also showed no requirement for *Myocd* for chimeric contribution to the atria.

During the time of this investigation another group published the effect of removing myocardin from common cardiac progenitor cells (Huang et al., 2012). Interestingly, *Nkx2-5*$^{Cre/+}$; *Myocd*$^{fl/fl}$ animals in their study displayed a much more severe phenotype resulting in embryonic lethality at E13.5. These animals exhibited myocardial hypolasia due to drastic increase in cardiomyocytes apoptosis and decrease of proliferation. These results parallel what is seen in our study in that *Myocd* is not required for progenitor cell differentiation into a cardiomyocyte fate, but is required for the survival and function of differentiated cardiac muscle. However, the detrimental effect of losing *Myocd* in embryonic cardiomyocytes was observed much earlier in development compared to our study. This discrepancy in phenotype onset is most likely is due to differences in genetic background as our study was on a mixed background as opposed to a congenic line.

Although the study by Huang et *al*. did not directly investigate smooth muscle differentiation and survival, it is worth noting that defects within the outflow tracts were not reported, despite the presence of cardiac progenitor-derived smooth muscle before E13.5. Given that our study additionally observes the presence of fully differentiated smooth muscle expressing smMHC at the base of the aorta in *Nkx2-5*$^{Cre/+}$; *Myocd*$^{fl/fl}$ animals, there is evidence that *Myocd* is not required for SHF-derived smooth muscle differentiation. This leads to two distinct possibilities in terms of the role *Myocd* may play in the development of cardiac progenitor-derived smooth muscle. One possibility is that *Myocd* is dispensable for differentiation, function and survival of aortic smooth muscle derived from the SHF. Both studies suggest, but cannot directly confirm this given the lack of specificity in the Cre lineage used.

Alternatively, while SHF-derived smooth muscle is present in *Nkx2-5*$^{Cre/+}$; *Myocd*$^{fl/fl}$ mutants, *Myocd* may be required for the survival of these cells similarly to cardiac muscle. This second scenario would mean that there would be a much more stringent requirement for *Myocd* in cardiomyocytes compared to smooth muscle, resulting in cardiomyocyte death and heart failure before an aortic phenotype can be observed. This represents an interesting question given the origin specific characteristics smooth muscle cells can exhibit (Majesky, 2007) and the findings that neural crest cell derived-smooth muscle within the ascending aorta require *Myocd* for differentiation and function (Huang et al., 2008).

Complications in testing this hypothesis arise from the fact that SHF-derived aortic smooth muscle shares the same Cre lineages used in cardiomyoctye studies. The ability to assay SHF-derived smooth muscle without the possibility of aortic defects arising secondary to heart failure may not be feasible *in vivo* at this time. *Ex vivo* experiments will also be complicated by the small population of SHF-derived smooth muscle relative to cardiomyocytes or smooth muscle from other embryonic sources. In the absence of more specific SHF markers or inducible SHF-Cre lines, newly developed *in vitro* models of origin specific smooth muscle differentiation (Cheung et al., 2012) may be one avenue to test the requirement for *Myocd* and other factors in smooth muscle differentiation from different embryonic lineages.

Methods and Materials

Mice and animal husbandry

This investigation conforms to the Guide for the Care and Use of Laboratory Animals published by the US National Institute of Health (NIH Publication No. 85-23, revised 1996). All animal protocols, experiments, and housing were performed following Institutional Approval for Appropriate Care and use of Laboratory animals by the UCLA Institutional Animal Care and Use Committee (Chancellor's Animal Research Committee (ARC)), Animal Welfare assurance number A3196-01.

The common cardiac / common second heart field progenitor lineage was traced with Cre knocked into one allele of the Nkx2-5 locus (*Nkx2-5*$^{Cre/+}$) (Moses et al., 2001). Atrial progenitors derived from the posterior SHF lineage were traced using transgenic Cre under the control of *sarcolipin* promoter elements (sln-Cre) (Nakano et al., 2011). Genetic removal of myocardin was achieved using a floxed allele of *myocardin* (*myocd*$^{fl/fl}$) (Huang et al., 2008). Noon of the day a vaginal plug was detected was considered embryonic day (E) 0.5. Noon of the day of birth was considered postnatal day (P) 0.

Histology and immunostaining

Embryo and neonatal sample preparations were performed as described previously (Harmon, and Nakano, 2013). H&E and Mason's Tri-Chrome staining were performed according to standard protocols. Section double staining with X-gal and specific antibodies were performed by staining slides with X-gal followed by post-fixation with 4%PFA for ten minutes. Antibody staining was then performed as described. Immunofluorescent and immunohistochemical stainings were performed as follows: 8-10μm fixed frozen sections were blocked with 10%

normal goat serum; 0.1% TritonX. Antibody reactions were carried out in 5% normal goat serum for one hour at room temperature or at 4 °C overnight. Fluorescent or peroxidase conjugated secondary antibody reactions were performed in 5% normal goat serum for one hour at room temperature. Immunofluorescent stainings were mounted with ProLong Gold DAPI media (Invitrogen). Alternatively, immunohistochemical development was performed through binding of ABC elite peroxidase conjugated avidin (Vectastain) and development with D.A.B substrate (Vector Labs) as described in the manufacturer's protocol.

Antibodies used and their working concentrations are as follows: mouse anti-cTnT (1:200, Lab Vision Corp., Fremont, CA), rabbit anti-smMHC (1:200, Biomedical Technologies Inc., Stoughton, MA), rabbit anti-sm22α (1:200, Abcam, Cambridge, UK), chicken anti-GFP (1:1000, Aves Labs, Tigard, OR), rat anti-Ter119 (1:100, eBioscience, San Diego, CA), rat anti-CD41 (1:50, BD Biosciences, San José, CA), rat anti-CD45 (1:50, BD Biosciences, San José, CA). For immunofluorescent detection the following Alexafluor conjugated secondary antibodies were used: goat anti-mouse-647, goat anti-chicken-488, goat anti-rabbit-594 (1:1000, Invitrogen, Grand Island, NY). For immunohistochemistry development goat anti-rabbit-biotin (1:1000, Invitrogen, Grand Island, NY).

Adenoviral Transduction

Atria from sln-Cre; $Rosa26^{LacZ/+}$ hearts were isolated and enzymatically dissociated at E12.5. Lineage traced atrial progenitors were plated on OP9 feeder cells and allowed to adhere for 18-24 hours. Co-cultures were incubated with an adenoviral vector containing an expression construct for *myocd*-flag or empty virus at a concentration of 10 MOI for 8 hours at 37 degrees and then washed off with PBS containing $Ca2^{+}$ and $Mg2^{+}$. Co-cultures were then tracked for 3 to

14 days before analysis. Infections were carried out in accordance with Bio Safety Level 2+ (BSL2+) practices.

Image analysis

Immunofluorescent imaging was performed on a Zeiss AxioImager system using Axiovision release 4.8. Confocal microscopy was performed on a Zeiss Laser Scanning Microscope (LSM) 780 system using the 2010 release of Zen image acquisition software. Colorimetric imaging was performed on an Olympus EX51 imaging system using DP2-BSW imaging software.

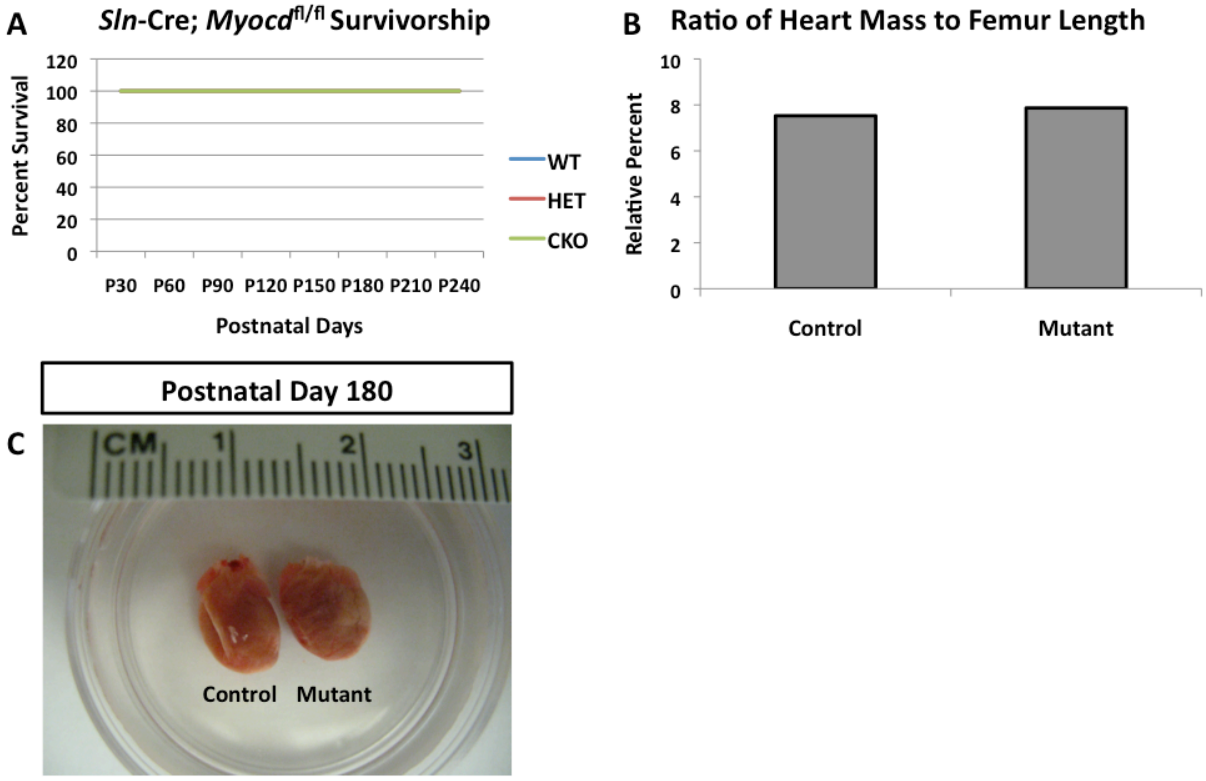

Figure 3-1: Myocd is not required for the development of cardiac structures derived from *Sln*$^{+}$ atrial progenitors. *Sln*-Cre ; *Myocd*$^{fl/fl}$ animals display normal life spans comparable to wildtype and heterozygote controls (A). Representative animals dissected at postnatal day 180 did not show signs of cardiac strain when heart mass was compared to femur length (B), and displayed normal heart size and morphology compared to wildtype controls (C).

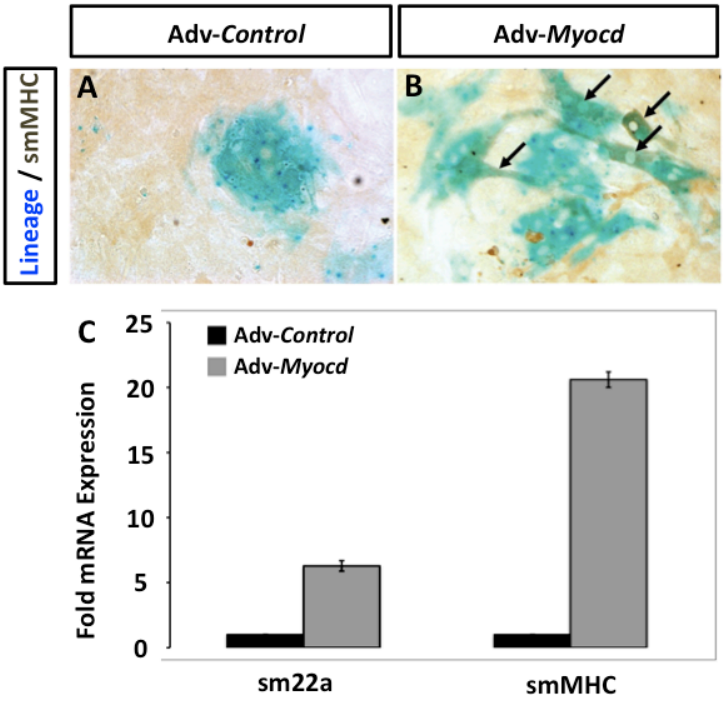

Figure 3-2: *Myocd* is sufficient to induce smooth muscle differentiation in *Sln*$^{+}$ atrial progenitors *ex vivo*. *Sln*-Cre ; Rosa26$^{LacZ/+}$ or *Sln*-Cre ; Rosa26$^{YFP/+}$ hearts were isolated at E12.5, enzymatically dissociated, plated on an OP9 mesenchymal feeder layer and infected with Adv-*Control* or Adv-*Myocd* adenoviral expression vectors. Cultured *Sln*$^{+}$ atrial progenitor cells (blue) treated with Adv-*Control* exhibit minimal spontaneous smooth muscle differentiation as indicated by expression of smMHC (mean 1%, A). Treatment of cultured progenitors with Adv-*Myocd* results in significantly increased expression of smMHC (mean 33%, B). YFP^{+} progenitors FACS purified and subjected to semi-quantitative PCR following treatment with the Adv-*Myocd* show increased mRNA expression of the smooth muscle markers sm22a and smMHC compared to progenitors treated with Adv-*Control* (C).

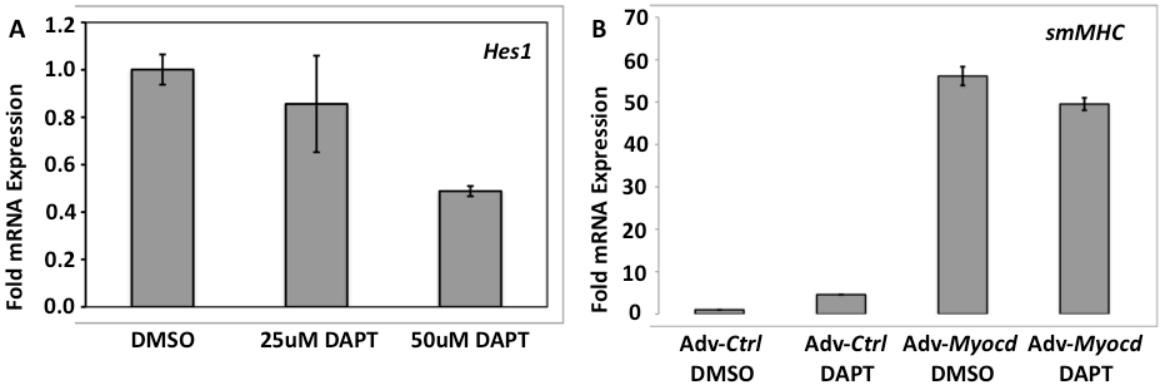

Figure 3-3: Inhibition of Notch signaling results in modest increases in smooth muscle marker expression in *Sln*$^{+}$ atrial progenitors. **(A)** *Sln*-Cre ; Rosa26$^{YFP/+}$ hearts were isolated at E12.5, enzymatically dissociated, plated on an OP9 mesenchymal feeder layer and treated with various concentrations of the Notch inhibitor DAPT. Treatment with a 50μM concentration of DAPT significantly decreases mRNA expression of the Notch reporter *Hes1* compared to vehicle control. **(B)** Treatment of cultured *Sln*$^{+}$ atrial progenitors with Adv-*Control* and 50μM DAPT modestly increased mRNA expression of smMHC compared to Adv-control and DMSO treatment. When DAPT is added to progenitors treated with Adv-*Myocd* there is no significant increase in smMHC expression compared to treatment with Adv-*Myocd* and DMSO vehicle.

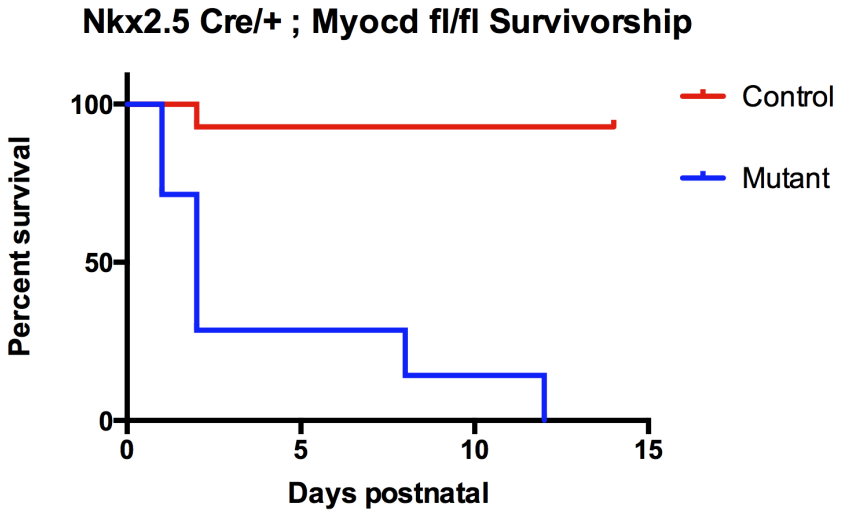

Figure 3-4: Conditional knockout of *Myocd* in early cardiac progenitors results in perinatal lethality. *Nkx2-5*$^{Cre/+}$; *Myocd*$^{fl/fl}$ animals are embryonic viable, but exhibit perinatal lethality with the majority of mutant animals dying at postnatal day 2 (P2).

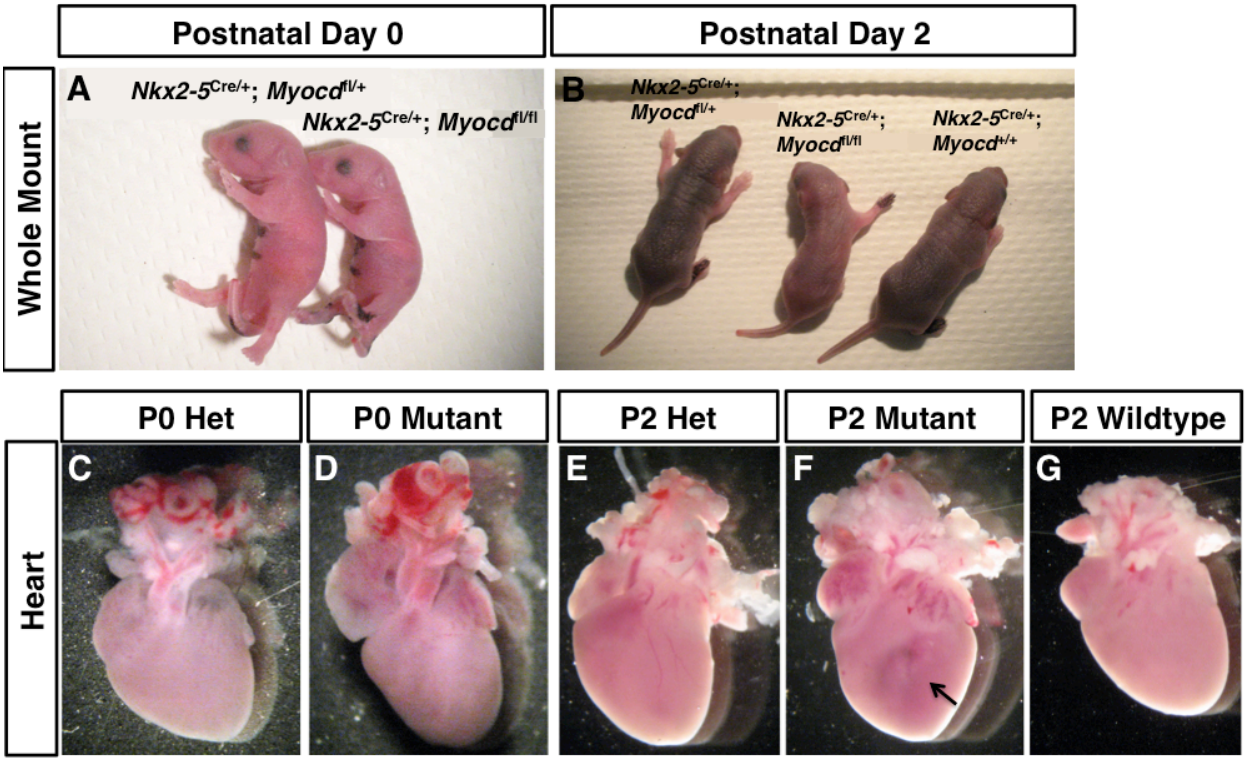

Figure 3-5: Conditional knockout of *Myocd* in early cardiac progenitors results in cardiac abnormalities at postnatal day two. *Nkx2-5*$^{Cre/+}$; *Myocd*$^{fl/fl}$ mutant animals show are modestly smaller than control littermates at postnatal day zero (P0), but otherwise appear phenotypically normal (A). At P0 mutant hearts (D) are unremarkable and of comparable size to control hearts (C). At postnatal day two *Nkx2-5*$^{Cre/+}$; *Myocd*$^{fl/fl}$ mutant animals are significantly smaller than control littermates exhibiting weakness and delayed pigmentation (B). Similarly to what is observed at P0, P2 mutant hearts (F) appear developmentally normal and of comparable size to controls (E,G), however discoloration and atypical morphology is observed within the ventricular myocardium (arrow).

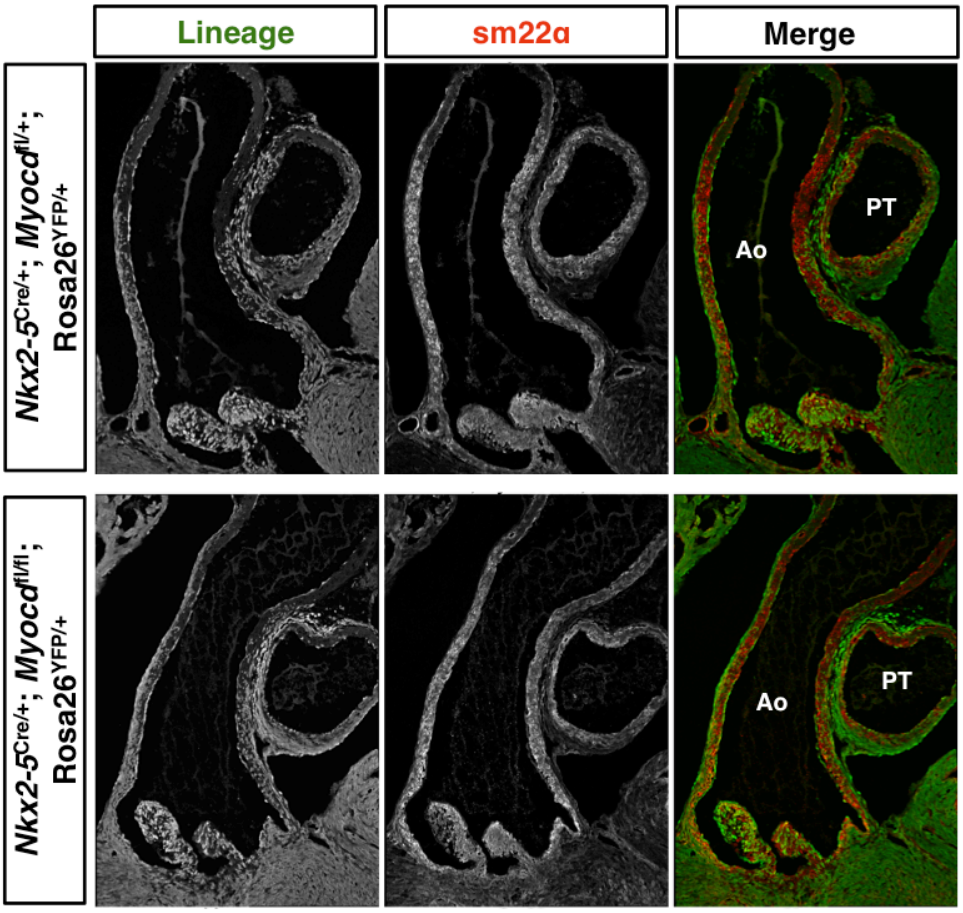

Figure 3-6: Outflow tract formation is not affected by loss of *Myocd* in early cardiac progenitors. Frontal sections were obtained from *Nkx2-5*$^{Cre/+}$; *Myocd*$^{fl/+}$; Rosa26$^{YFP/+}$ (top panel) and *Nkx2-5*$^{Cre/+}$; *Myocd*$^{fl/fl}$; Rosa26$^{YFP/+}$ (bottom panel) P2 hearts. Sections bisecting the transverse plane of the aorta were co-stained for YFP (left, green) and the smooth muscle marker sm22α (middle, red). Correct expression of sm22α is observed throughout the aortic media of both mutant and control hearts. Normal vessel dilation and contribution of *Nkx2-5*$^{+}$ progenitors is observed within the endothelium, media and valves of mutant aortas.

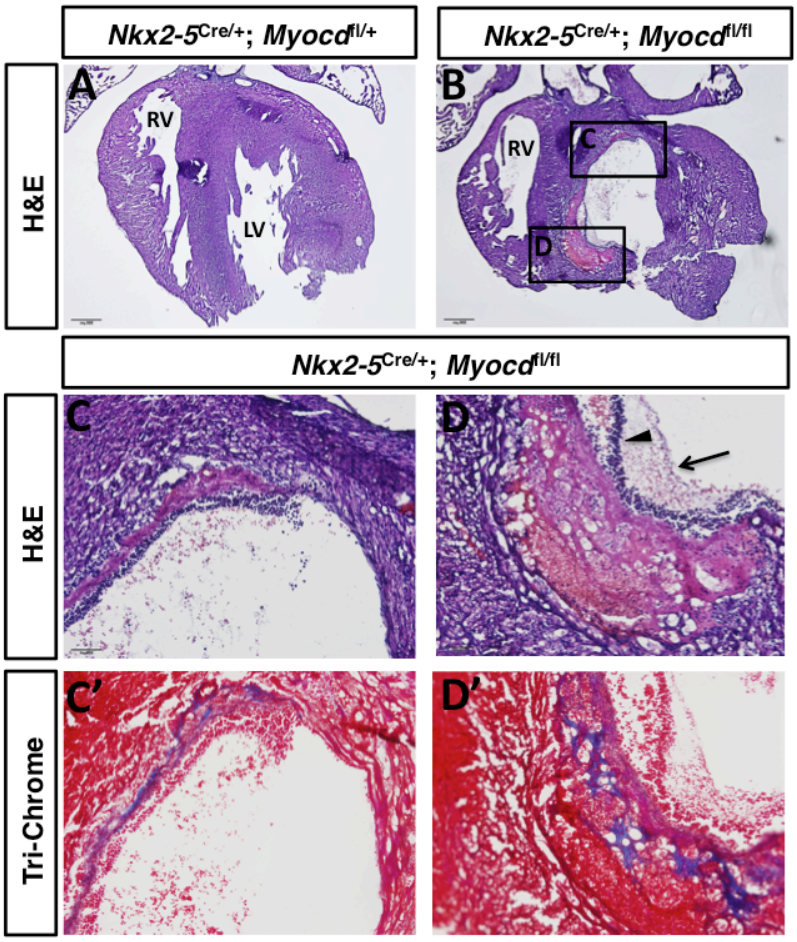

Figure 3-7: Loss of Myocd in early cardiac progenitors results in lesions and fibrosis within the neonatal myocardium. Frontal sections of P2 hearts from *Nkx2-5*$^{Cre/+}$; *Myocd*$^{fl/+}$ (A) and *Nkx2-5*$^{Cre/+}$; *Myocd*$^{fl/fl}$ (B-D) were histologically stained. H&E staining shows normal basophilic staining of the ventricular myocardium in control hearts (A) while conditional mutants display cardiac lesions composed of ectopic eosinophillic tissue along the septal wall of the left ventricle (B). High magnification of mutant hearts reveals enucleated (arrow) and nucleated (arrowhead) blood cells adhering to the lesion (C,D). Mason's Tri-Chrome staining of sister sections reveals ectopic collagen deposition (blue) within the lesion (C', D').

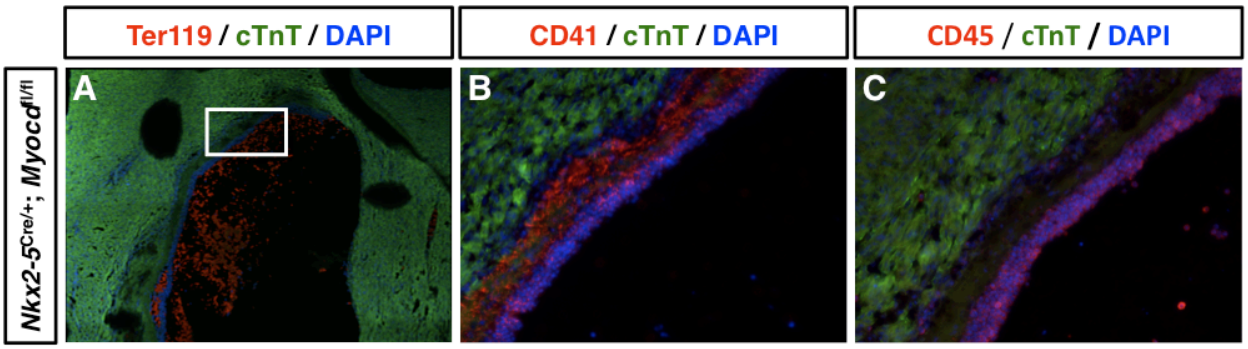

Figure 3-8: Cardiomyocyte fibrosis leads to blood aggregation and mural thrombus.

Frontal sections of P2 hearts from *Nkx2-5*$^{Cre/+}$; *Myocd*$^{fl/fl}$ were stained for blood lineage surface markers (red), the cardiomyocyte marker cTnT (green) and the nuclear dye DAPI (blue). Staining with Ter119 shows that the enucleated cells seen proximal to fibrotic mutant myocardium are erythrocytes (A). CD41 staining shows extensive aggregations of platelets within the lesion (B), while CD45 staining identifies the nucleated blood cells adhering to the chamber wall as leukocytes (C).

CHAPTER FOUR:

The Role of Inhibitory Smads in the Embryonic Heart

Introduction

Within the developing heart, cross talk between the endocardium and myocardium is essential for the proper formation of structures derived from both cell layers. This includes formation of the cardiac cushions of the atrio-ventricular canal (AVC) and outflow tract (OFT) that will ultimately form the valves of the heart. Cushion formation begins at E9.5 in mice, with a subset of cushion endocardial cells being activated and undergoing epithelial to mesenchymal transition (EMT). The process of endocardial EMT is highly dependant on cell non-autonomous signals from the surrounding cushion myocardium. *In vitro* invasion assays have shown the specificity of the interaction between myocardium underlying the OFT and AVC and presumptive cushion endocardium. While myocardium isolated from the cushion regions is sufficient to induce EMT in culture cushion endocardium *ex vivo*, the same experiment performed with ventricular cardiomyocytes elicits no response from endocardial cells (Runyan and Markwald, 1983; Mjaatvedt et al., 1987). The cell non-autonomous factors required for endocardial EMT include specific extracellular matrix (ECM) molecules secreted from the cushion myocardium as well as Transforming Growth Factor Beta (TGF-ß) and Bone Morphogenetic Protein (BMP) signaling ligands that reside within the cushion's ECM and act on endocardial cells.

Within the developing mouse heart TGF-ß2 expression is restricted to the OFT and AVC, and only expands after the completion of EMT at the cushions (Dickson et al., 1993). The functional necessity for TGF-ß2 has been illustrated with both gain- and loss-of-function experiments. Treatment of *ex-vivo* cushion endocardium with TGF-ß2 blocking antibodies inhibits their activation (Camenisch et al., 2002). Treatment of cushion endocardial explants with BMP2 is sufficient to induce EMT with or without co-culture with cushion myocardium. BMP2 treatment also resulted in increased expression of TGF-ß demonstrating crosstalk between

TGF-ß superfamily members within the endocardium (Sugi et al., 2004). Analysis of multiple models of cardiac specific BMP4 loss-of-function suggests that BMP4 is not required for the initiation of EMT within the cushion endocardium, but promotes cell proliferation within the cardiac cushions downstream of EMT activation (Jiao et al., 2003; McCulley et al., 2008) .

Within the TGF-ß superfamily, ligand binding activates receptor-regulated Smad proteins (R-Smads) via phosphorylation. These activated R-Smad complexes, Smad1/5/8 in the BMP pathway and Smad2/3 in the TGF-ß pathway, are then able to bind to Smad4 within the cytosol. Smad4/R-Smad complexes then translocate into the nucleus and activate a transcriptional signaling response (Moustakas et al., 2001). This intracellular activation cascade is not only necessary for the relay of ligand based signaling to the nucleus, but also adds an additional opportunity for signal regulation. Within the cytoplasm of BMP and TGF-ß receiving cells, Smad6 and Smad7 act as signal attenuators by interfering with Smad4 dependant signal transduction. These inhibitory Smads (iSmads) are structurally similar to other Smad proteins, but lack a C-terminal phosphorylation motif (Whitman 1997 reference). Within the cell Smad6 is able to inhibit BMP signaling by stably interacting with type1 BMP receptors to prevent the phosphorylation of Smad1 (Imamura et al., 1997; Nakayama et al., 1998) and additionally by sequestering activated phospho-Smad1 before it can bind to Smad4 (Hata et al., 1998). Through these interactions Smad6 is able to prevent the formation of the Smad4/R-Smad complex necessary for a transcriptional response within the nucleus.

In addition to repressing BMP signaling in a similar fashion to Smad6, Smad7 also stably interacts with type 1 TGF-ß receptors, blocking the phosphorylation of Smad2 and preventing the formation of the Smad4/R-Smad complex necessary for TGF-ß signal propagation (Hayashi et al., 1997; Nakao et al., 1997). It is also known that activation of canonical TGF-ß signaling

can induce the expression of inhibitory Smad7 suggesting a negative-feedback loop to adjust signal response (Nakao et al., 1997).

The role of Smad6 in the heart has previously been assessed by global genetic knockout. *Smad6* mutants on a mixed genetic background exhibit adult outflow tract defects including advanced ossification and cartilaginous metaplasia of the aortic media. The valves of adult mutants also exhibit striking valve hyperplasticity (Galvin et al., 2000). While this knockout study shows the only loss-of-function model resulting in ectopic valve enlargement, the mechanism that accounts for this striking phenotype has never been investigated. Given that *Smad6* is expressed within the endocardial cushions early in heart development it could play an active role in regulating the number of endocardial cells that undergo EMT and maintaining the proper developmental window in which EMT can occur. Smad6 expression is also maintained throughout development (Galvin et al., 2000), indicating the possibility that it is involved in regulating mesenchymal cell proliferation during valve formation and remodeling. Further, a recent study in the zebrafish model suggests a possible Smad6-mediated mechanism of SHF-progenitor differentiation in the outflow tract (de Pater et al., 2012). However, this has not been addressed within a murine model and could relate to BMP associated congenital OFT defects.

Interestingly, *Smad7* has overlapping expression patterns with *Smad6* within the cushion endocardium (Snider et al., 2009), but does not produce a valve phenotype in loss-of-function studies. Previous studies have analyzed mice homozygous for *Smad7* hypomorphic alleles created through targeted deletion of the MH2 domain. These $Smad7^{\Delta MH2/\Delta MH2}$ animals contain embryonic ventricular septal defects as well as non-compaction of the ventricular myocardium, both resulting from increased TGF-ß signaling in the AV cushions and ventricular endocardium respectively (Chen et al., 2009).

Currently, the differences in phenotypes between *Smad6* and *Smad7* loss-of-function models suggest that these proteins have non-overlapping roles, despite being co-expressed within cushion endocardium during development (Yamada et al., 1999; Snider et al., 2009; Galvin et al., 2000) and having similar mechanisms of action (Massagué et al., 2005). However, previous functional studies of iSmads in cardiogenesis were performed on separate mixed genetic backgrounds and presented with variable phenotypic penetrance. Combining *Smad6* knockout and *Smad7* ΔMH2 alleles on the same congenic background could serve to address both functional overlap between iSmad molecules as well as examine embryonic phenotypes that may not be observed in outbred strains.

Here we use double heterozygotes containing Smad6 knockout and Smad7 ΔMH2 alleles bred onto a congenic C57/Bl6 genetic background to investigate the role iSmads play embryonically in regulating endocardial EMT and valve proliferation. Our initial results show that on a strict congenic background *Smad6* knockout results in embryonic valve hyperplasia as early as E12.5, exhibiting increased levels of Snail within the cushion endocardium. *Smad6* mutants also exhibit novel embryonic congenital defects including double outlet right ventricle. Additionally, a single *Smad7* ΔMH2 allele in the *Smad6* mutant background increases gross cardiac phenotype severity. Taken together our results suggest that Smad6 may specifically control early EMT in the cushion endocardium to regulate down stream valve size and function.

Results

Expression of *Smad6* and *Smad7* in the embryonic heart

Previous research has shown adult phenotypes related to cushion development when normal iSmad function is lost (Galvin et al., 2000; Chen et al., 2009). In order to investigate potential roles these proteins may play in earlier development we determined their expression during embryogenesis by section *in situ* hybridization. At E10.5 *Smad6* and *Smad7* mRNA is abundantly co-expressed within both endocardial and mesenchymal cells of the AVC cushion (Figure 4-1 A, B) and OFT cushion (Figure 4-1 C, D).

To investigate a potential role for Smad6 in SHF-progenitor differentiation we compared the expression of *Smad6* to the expression of the SHF marker *Isl1*. At E10.5 *Isl1* mRNA is robustly expressed in distal populations of SHF progenitor cells and migratory SHF progenitors within the pharyngeal arches proximal to the anterior pole of the heart (Figure 4-1 F). *Smad6* mRNA co-localizes with *Isl1* expression within SHF cells within the pharyngeal mesoderm, but not with less differentiated distal progenitors (Figure 4-1 E). At E9.5, in addition to being expressed within the prospective cushion endocardium, *Smad6* is expressed within the myocardium at the distal end of the developing outflow tract (Figure 4-1 H). Staining for *Isl1* mRNA confirms that *Smad6* is expressed where SHF progenitor cells have entered the elongating heart tube, but have not fully differentiated into myocardium (Figure 4-1 I). Taken together this expression data suggests a potential role for iSmads in regulating both early EMT events in the endocardium as well as proliferation in the cushion mesenchyme. Expression of *Smad6* within the distal OFT myocardium suggests a conserved role in cardiac progenitor differentiation as previously described within the zebrafish model (de Pater et al., 2012).

Loss of iSmad function leads to congenic outflow tract defects during embryogenesis

To determine iSmads play a role in embryonic heart development, we crossed *smad6*$^{+/-}$; *smad7*$^{+/\Delta MH2}$ double heterozygote animals bred on a congenic C57/Bl6 background. Given our interest in endocardial EMT and valve formation our initial focus was on *Smad6* knockouts animals. In contrast to the previous study where *Smad6* mutants survived to adulthood, our breedings observed no *smad6* mutants neonatally, suggesting embryonic lethality. In addition to *Smad6*$^{-/-}$, *Smad6*$^{-/-}$; *Smad7*$^{+/\Delta MH2}$ and *Smad6*$^{-/-}$; *Smad7*$^{\Delta MH2/\Delta MH2}$ animals were not observed at postnatal day 0 (P0).

Analysis at E15.5 shows that *Smad6* mutant embryos exhibit modest size variation, but appear otherwise phenotypically normal compared to control littermates (Figure 4-2 A, B). While E15.5 *Smad6* mutant hearts are of comparable size to controls, they exhibit the congenital outflow tract defect double outlet right ventricle (DORV) (Figure 4-2 A', B'). This defect is characterized by the misalignment of the outflow tracts resulting in both the aorta and pulmonary trunk connect to the right ventricle. Histological analysis of mutant hearts confirms the connection of both outflow tracts to the right ventricle in mutants (Figure 4-2 B'') compared to the single connection to the pulmonary trunk seen in littermates (Figure 4-2 A''). At this timepoint we observed *Smad6*$^{-/-}$; *Smad7*$^{+/\Delta MH2}$ embryos that exhibited characteristics of impaired cardiac function including subcutaneous edema along the dorsal length of the embryo in addition to discoloration of the liver (Figure 4-2 C). Morphological analysis of *Smad6*$^{-/-}$; *Smad7*$^{+/\Delta MH2}$ hearts showed a single outflow tract leading from the right ventricle (Figure 4-2 C'). Histological analysis of this outflow tract determined that *Smad6*$^{-/-}$; *Smad7*$^{+/\Delta MH2}$ animals also exhibit DORV and that the outflow vessel seen within whole mount pictures is both the aorta and

pulmonary trunk surrounded by ectopic adventitial tissue (Figure 4-2 C''). *Smad6*$^{-/-}$; *Smad7*$^{\Delta MH2/\Delta MH2}$ mutants were not observed at E15.5.

Loss of iSmad function leads to embryonic valve hyperplasia

To determine if the valve hyperplasia seen in previous *Smad6* studies represents a proliferative defect after valve formation is completed or represents ectopic levels of EMT, we have begun to analyze the role of Smad6 within embryonic valve development. At E15.5 *Smad6* mutants exhibit significant valve hyperplasia of the mitral, tri-cuspid and pulmonary valve of the DORV out-flow tract compared to wildtype controls (Figure 4-3 middle, top). *Smad6*$^{-/-}$; *Smad7*$^{+/\Delta MH2}$ also display valve hyperplasia of the pulmonary valve with more variable hyperplasticity within the mitral and tri-cuspid valves (Figure 4-3 bottom). To directly test whether ectopic cushion endocardium activation could be responsible for increases in valve size, we analyzed the expression of the EMT marker Snail. At E10.5 *Smad6*$^{-/-}$ OFT cushion exhibited increased numbers of Snail^{+} cells within the endocardium with comparable numbers of Snail^{+} mesenchymal cells within the developing cushion (Figure 4-4 A, B). Taken together these findings suggest that valve hyperplasia due to loss of *Smad6* is not primarily due to a prolonged defect during the lifespan of mutants, but presents early in valve formation during embryogenesis. Further, ectopic EMT represents one potential mechanism for this phenotype.

Discussion

Here we describe novel embryonic phenotypes associated with loss of *Smad6*. We show that on a strict C57/Bl6 genetic background *Smad6* mutants exhibit embryonic lethality and novel embryonic phenotypes, including early on-set valve hyperplasia and the congenital defect double outlet right ventricle. Our study shows that ectopic EMT may be a possible cause for embryonic valve hyperplasticity and correlative evidence that the outflow tract defects we observe could be due to a role for *Smad6* in SHF progenitor differentiation. Finally, our study provides a platform for looking at whether Smad6 and Smad7 have independent or shared functions within the cushion endocardium and mesenchyme through the creation of compound iSmad loss-of-function embryos.

The previous observation of post-embryonic valve hyperplasia in adult *Smad6* mutant animals (Galvin et al., 2000) leaves several unaddressed questions concerning the molecular events responsible for this phenotype. If endocardial cushions and nascent cardiac valves showed no phenotypical differences in size, then it would suggest that aberrant cell proliferation within the valve mesenchyme after formation is responsible. While the state of mutant embryonic tissue was not reported in the initial smad6 study, our observation of hyperplasia directly following valve morphogenesis raises the possibility that ectopic EMT in cushion endocardium could be the driving factor. Our data further supports this hypothesis showing increased numbers of endocardial cells expression the EMT marker Snail in *Smad6* mutant OFT endocardium. However, this does not rule out the contribution of ectopic proliferation within cushion mesenchyme or the nascent valves.

A recent zebrafish study describes an additional role for iSmads within the embryonic heart, showing *smad6* is required to down regulate BMP signaling in cardiac-progenitors as they

enter the OFT (de Pater et al., 2012). In mice, disruption of SHF-dependant OFT elongation and the subsequent maturation of cardiomyocytes within the truncus have been linked to several types of congenital defects including DORV (Ward and Kirby, 2006). mRNA expression of *Smad6* within the distal myocardial layer of the developing OFT raising the possibility that Smad6 serves a conserved role in the differentiation of the anterior SHF in mammals. However, direct evidence for this has yet to be investigated.

The results discussed in this chapter represent only the initial findings of an ongoing research study. While taken together our results show that Smad6 may be required earlier in development than previously described, within both the cushion endocardium and OFT myocardium, several important experiments remain to be performed. Therefore, immediate and long term goals of this study will be discussed in detail within Chapter Five.

Methods and Materials

Mice and animal husbandry

This investigation conforms to the Guide for the Care and Use of Laboratory Animals published by the US National Institute of Health (NIH Publication No. 85-23, revised 1996). All animal protocols, experiments, and housing were performed following Institutional Approval for Appropriate Care and use of Laboratory animals by the UCLA Institutional Animal Care and Use Committee (Chancellor's Animal Research Committee (ARC)), Animal Welfare assurance number A3196-01.

Mice harboring a *smad6* knockout allele (Galvin et al., 2000) were intercrossed with mice containing a *smad7* ΔMH2 loss-of-function allele (Chen et al., 2009) to create double heterozygotes before being backcrossed to genetic uniformity on a C57/Bl6 background. Double heterozygote animals were bred to creat single and compound loss of iSmad function embryos. Noon of the day a vaginal plug was detected was considered embryonic day (E) 0.5. The day when newly born pups were discovered was considered postnatal day (P) 0.

Histology and immunostaining

Embryo and neonatal sample preparations were performed as described previously (Harmon, and Nakano, 2013). H&E staining was performed according to standard protocols. Immunofluorescent stainings were performed as follows: 8-10μm fixed frozen sections were blocked with 10% normal goat serum; 0.1% TritonX. Antibody reactions were carried out in 5% normal goat serum for one hour at room temperature or at 4 °C overnight. Fluorescent conjugated secondary antibody reactions were performed in 5% normal goat serum for one hour at room temperature. Slides were mounted with ProLong Gold DAPI media (Invitrogen).

Antibodies used and their working concentrations are as follows: rat anti-CD31 (1:100, BD Biosciences, San José, CA), rabbit anti-Snail (1:200, Cell Signaling, Boston, MA). For immunofluorescent detection the following Alexafluor conjugated secondary antibodies were used: goat anti-chicken-488, goat anti-rabbit-594 (1:1000, Invitrogen, Grand Island, NY).

Section in situ hybridization

In situ hybridization on 10uM cryosections was performed as desribed in (Pearson et al., 2011).

Image analysis

Immunofluorescent imaging was performed on a Zeiss AxioImager system using Axiovision release 4.8. Confocal microscopy was performed on a Zeiss Laser Scanning Microscope (LSM) 780 system using the 2010 release of Zen image acquisition software. Colorimetric imaging was performed on an Olympus EX51 imaging system using DP2-BSW imaging software.

Figure 4-1 Expression of iSmads during early cardiac development.

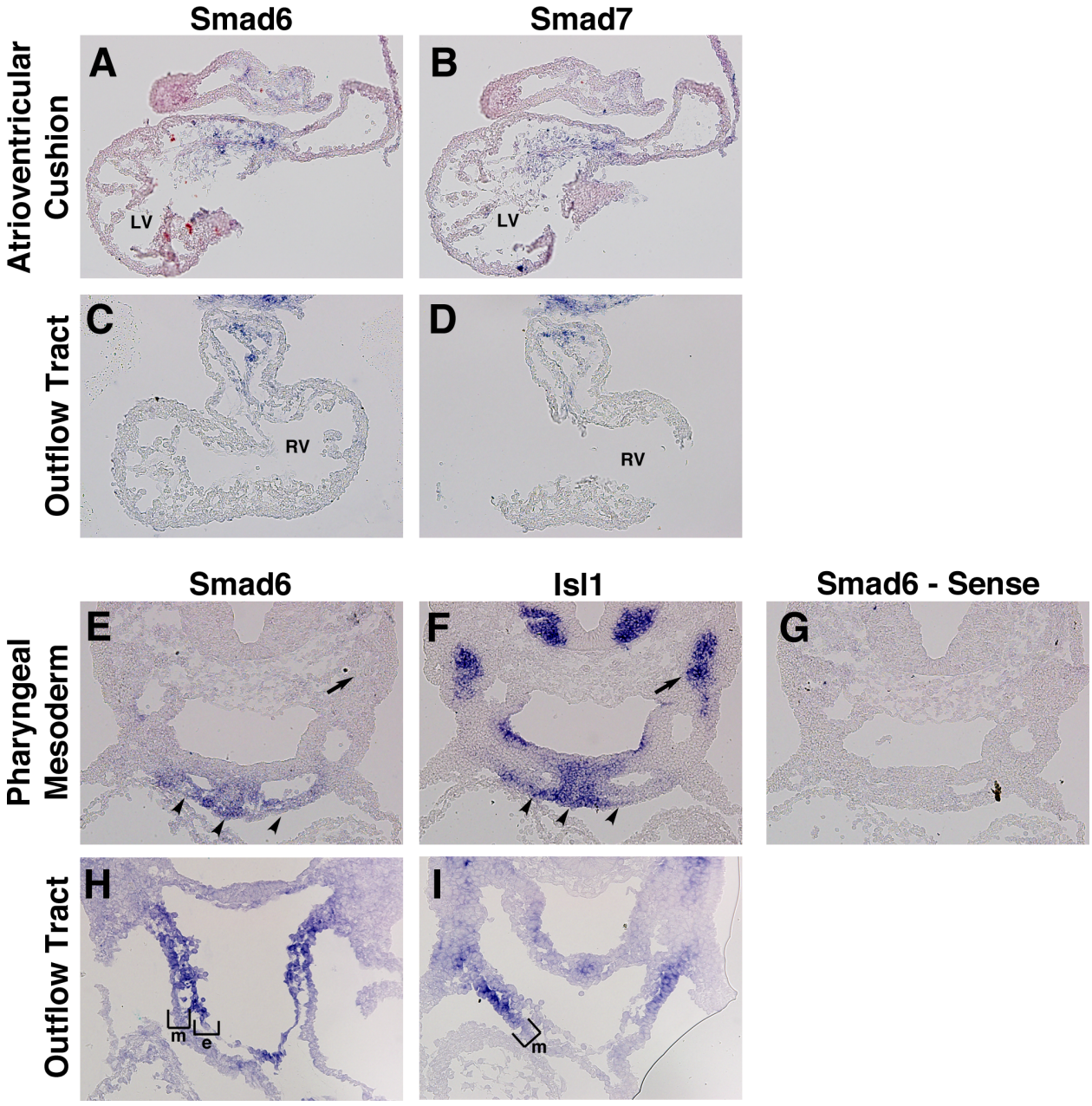

Figure 4-1 Expression of iSmads during early cardiac development.

In situ hybridization of transverse sections from E10.5 **(A-G)** and E9.5 **(H,I)** wildtype embryos. *Smad6* and *Smad7* have a shared expression domain within both cushion endocardium and mesenchyme of the atrioventricular canal (A,B) and outflow tract (B,C). *Smad6* expression co-localizes with the SHF marker *Isl1* within the pharyngeal mesoderm (E,F, arrowheads), but not within distal populations of SHF progenitors (E,F, arrows). Control sense reaction demonstrates hybridization specificity (G). *Smad6* expression co-localizes with the SHF-marker *Isl1* within distal OFT myocardium (H,I, bracket). a – atria, e – endcardium, lv – left ventricle, m – myocardium, rv – right ventricle.

Figure 4-2: Loss of iSmad function results in embryonic cardiac phenotypes

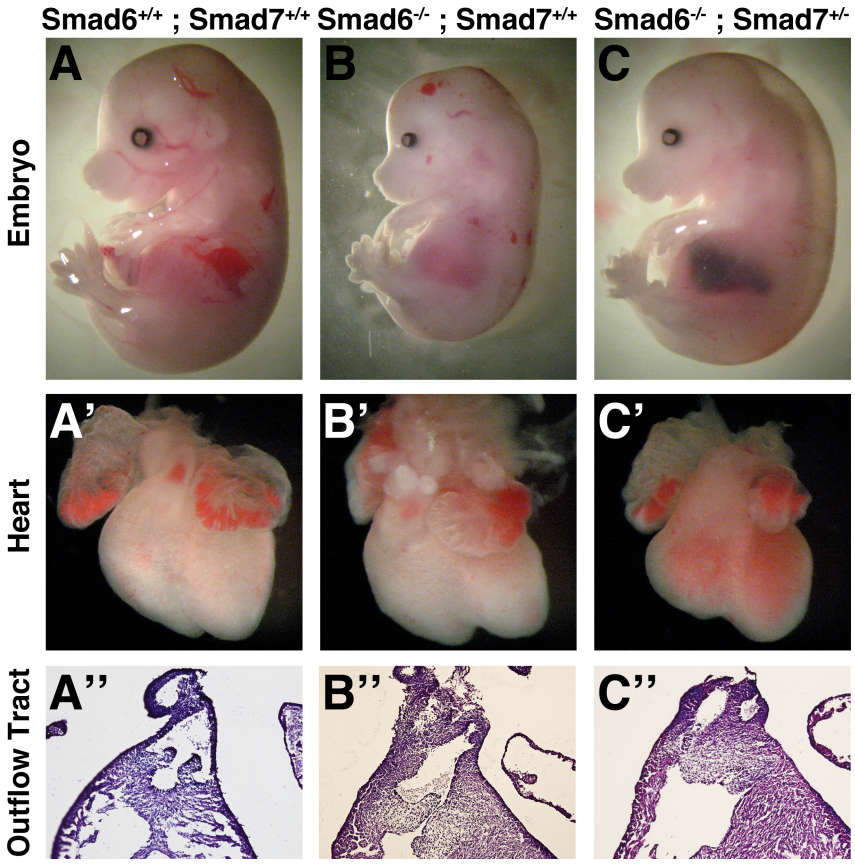

Figure 4-2: Loss of iSmad function results in embryonic cardiac phenotypes

(A-C) Whole mount images of E15.5 embryos from crossing *Smad6*$^{+/-}$; *Smad7*$^{+/\Delta MH2}$ double heterozygote animals. *Smad6* mutant embryos show slight variation in size, but look phenotypically normal (B). *Smad6* mutants with an additional *Smad7* hypomorphic allele have characteristics of impaired heart function including subcutaneous edema along the spine and darkening of the liver (C). **(A'-C')** Whole mount images of E15.5 hearts corresponding to embryos shown in (A-C). At E15.5 the outflow tract is septated and the aorta and pulmonary trunk are aligned to the correct ventricles (A'). *Smad6* mutant hearts display the congenital defect double outlet right ventricle (DORV)(B'). *Smad6* mutant hearts with an additional *Smad7* hypomorphic allele also display DORV with ectopic adventitia surrounding both outflow tracts (C'). **(A''-C'')** Section H&E staining of E15.5 hears corresponding to embryos shown in (A-C). Histology of sections through the outflow tract confirms septation of defective outflow tracts and congenital DORV (B'',C'').

Figure 4-3: Loss of iSmad function leads to embryonic valve hyperplasia

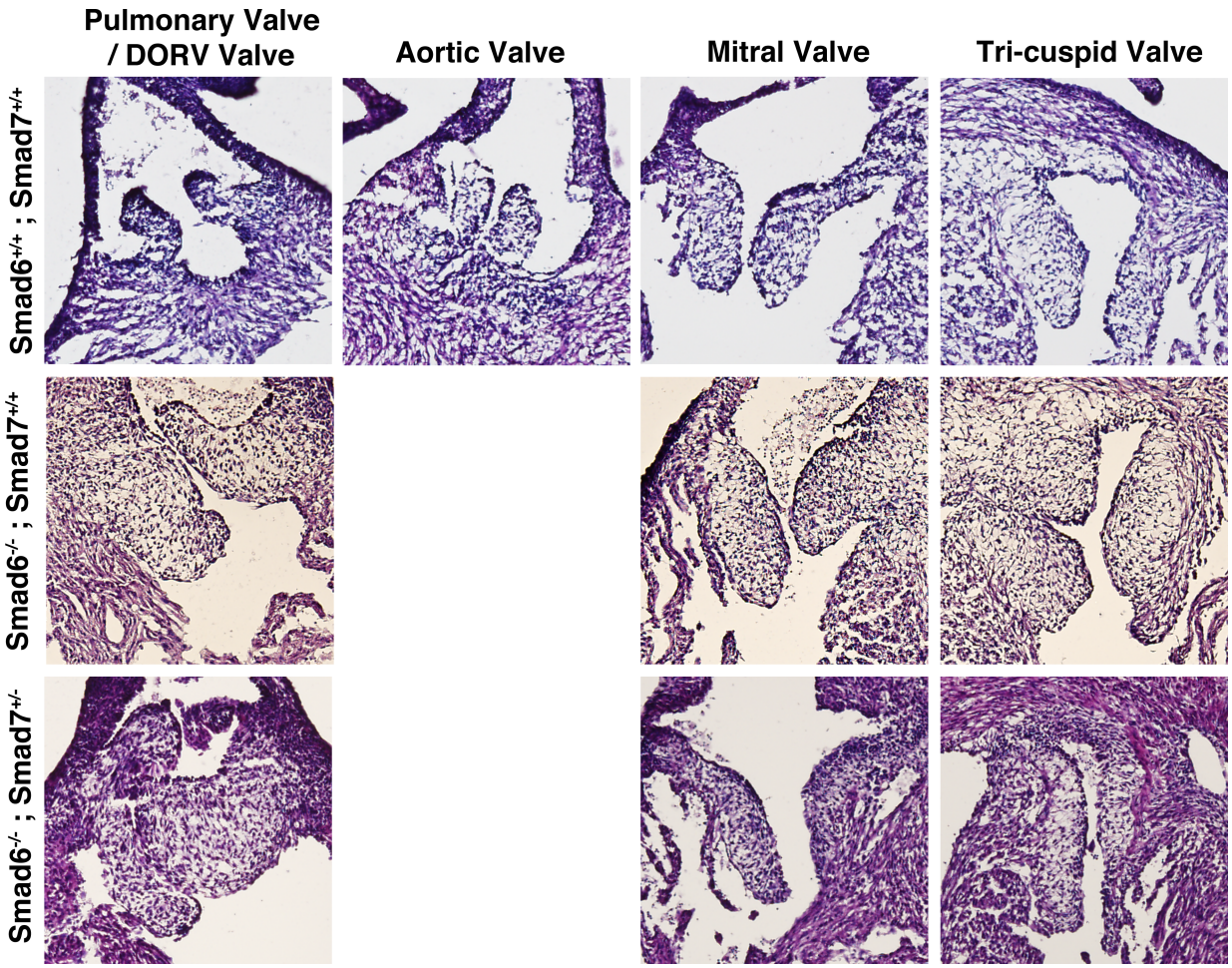

Figure 4-3: Loss of iSmad function leads to embryonic valve hyperplasia.

Sections of E15.5 hearts from crossing *Smad6*$^{+/-}$; *Smad7*$^{+/\Delta MH2}$ double heterozygote animals were H&E stained to show cardiac valve morphology. By E15.5 the four cardiac valves have formed in wildtype animals (top). *Smad6* mutant hearts show embryonic valve hyperplasia of the DORV outflow tract, mitral and tricuspid valves (middle). *Smad6* mutant hearts with an additional *Smad7* hypomorphic allele also display hyperplasia of the DORV outflow tract valve with variance in size of the mitral and tricuspid valves (bottom).

Figure 4-4: Loss of *Smad6* results in increased Snail expression in cushion endocardium

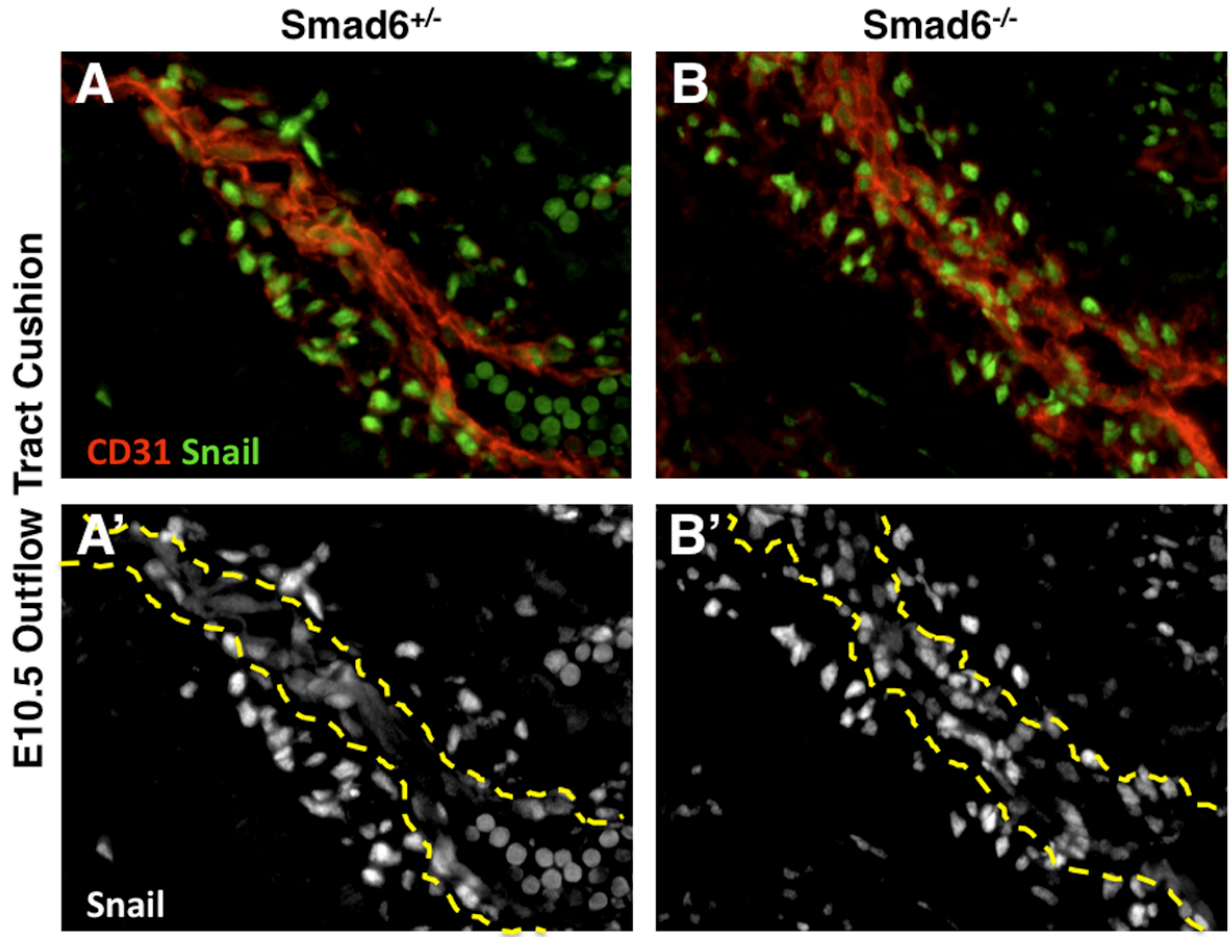

Figure 4-4: Loss of *Smad6* results in increased Snail expression in cushion endocardium

Sagital sections of *Smad6* heterozygote and mutant embryos were co-stained with antibodies for the endothelial marker CD31 (red) and the EMT marker Snail1 (green). While the majority of cells within the cushion express Snail, loss of *Smad6* results in increased Snail expression within endocardial cells of the OFT (B,B') compared to control tissue (A,A'). dashed line – boundary between endocardium and underlying cushion mesenchyme

CHAPTER FIVE:

Concluding Remarks

Summary

The work presented in this dissertation focuses on signaling events that regulate the formation and maturation of the embryonic heart. Our studies focus on the development of diverse structures derived from second heart field progenitors including: the media layer within the base of the aorta, the ventricular myocardium and the cardiac valves. This work highlights the importance of specialized non-cardiac structures within the developing heart and their relationship to the underlying myocardium. In Chapter 2, we describe the anatomical boundaries of SHF-derived smooth muscle and the boundary it forms with neighboring cells derived from the Neural Crest. Chapter 3 describes a differential requirement for the SRF co-factor *Myocd* in SHF-derived smooth muscle and cardiomyocyte development and survival. Chapter 4 describes the role of Smad6 in regulating BMP signaling within endocardial cushion formation and early valve development. While SHF-derived smooth muscle and cushion mesenchyme represent small cellular populations, their development is critical and is associated with a host of congenital cardiac defects. In Chapter 5, possible future studies will be discussed as well as the clinical implications of our work.

Origin specific characteristics of SHF-derived smooth muscle

Myocd is a unique regulatory molecule given its dual role in cardiac and smooth muscle regulation. While a similar study from the Paramcek group confirms and expands on our findings concerning the role of Myocd in cardiomyocyte survival, many important questions remain about the signaling factors required for development of SHF-derived smooth muscle.

Within the vascular biology field, growing interest centers on whether smooth muscle cells (SMCs) from different origins exhibit functionally distinct characteristics, despite their

common role and indistinguishable morphology. Initial studies in chick have shown a striking difference when labeled SMCs from the neural crest-derived ascending aorta and the splanchnic mesoderm-derived thoracic aorta were treated with TGF-ß *in vitro* (Topouzis and Majesky, 1996). These included opposite responses in auto-induction of TGF-ß, proliferation, and contraction. In addition to determining specifically how adult smooth muscle from different sources responds to extracellular signals, important information can be gained by determining whether mechanisms of SMC development are conserved or unique.

Our study was unable to directly determine whether or not *Myocd* (and SRF signaling) is required for SHF-derived smooth muscle development. This was due to SHF-derived smooth muscle and myocardium both being labeled by *Nkx2-5*-Cre. Given *Myocd*'s association with cardiomyocyte survival and the role in plays in the differentiation and function of neighboring neural crest-derived smooth muscle it remains an important question worth addressing. While assaying whether specific factors are required in smooth muscle differentiation from the SHF may not be feasible *in vivo* given the obstacles described in Chapter 2 and 3, a recent *in vitro* model of SMC differentiation (Cheung et al., 2012) may provide a new tool for these studies. Using the protocol developed by Cheung *et* al., unbiased screens could be performed on ES-derived lateral plate mesodermal intermediates to determine what factors are essential for *in vitro* smooth muscle differentiation. In addition, key factors already known to be important within the neural crest, such as *Myocd*, could be selectively tested within the SHF in this *in vitro* screen.

Related to these studies is the hypothesis that an incoherent response from two different groups of adjacent smooth muscle may underlie pathologies associated with the aortic media such as dissection. While several groups have raised this interesting hypothesis, it has yet to be directly tested. A logical next step in our study of mapping the anatomical distribution of SHF-

derived smooth muscle would be to track the location and incidence of dissection in relationship to smooth muscle boundaries. Given that aortic smooth muscle from different embryonic origins is histologically indistinguishable, the most feasible way to accomplish this would involve animals with a lineage tracer of one of the four sources of aortic smooth muscle in their genetic background. Cre/Lox lineage traced animals could then be assayed in combination with chemical induction of dissection (Gong et al., 2006) or induction of dissection using additional genetic alleles (Faugeroux et al., 2013). We speculate that the boundary between SHF and Neural Crest Cell-derived smooth muscle represents the most critical transition within the aorta due to the increased level of pulsatile stress it encounters in proximity to the contracting ventricles.

The role of iSmads in endocardial cushion development

Valvulogenesis is a complex process that involves endocardial cushion formation in the early embryo, proliferation and remodeling of cushion mesenchyme and maturation of the nascent valve structures. While our study shows that *Smad6* is required within the early embryo for normal valve development, several questions regarding the specific role it plays remain unanswered. To further this study it will be necessary to directly confirm that the embryonic valve hyperplasia observed in *Smad6* mutants is due to increased level of activated BMP signaling. This can be visualized by staining for phosphorylated Smad1/5/8, ideally at E15.5, as well as earlier time points when EMT is being initiated. While the literature suggests that smad6 preferentially down regulates BMP signaling and is not involved in the TGF-b pathway (Shi and Massagué, 2003), comparing the levels of activated TGF-ß signaling via phosphorylated Smad2/3 staining would also be an appropriate control.

The other fundamental question that should be addressed in the continuation of this study is whether valve hyperplasia is caused by ectopic EMT or increased proliferation of mesenchymal cells. We have begun to address this question using Snail as an early EMT marker, but proliferation of cushion mesenchyme should be assayed at several embryonic timepoints via staining for phosphorylated histone H3 or a more sensitive method such as BrdU labeling. Other immediate aims include determining the exact age of embryonic lethality and the earliest time point in which endocardial signal response is altered. Further, determining critical gene targets in the endocardium whose expression is incompatible with high BMP signaling would provide novel mechanistic insights into the function of *Smad6* in the context of valve development. This could be done via microarray or next generation sequencing.

This portion of the dissertation also lays the foundation for several novel follow-up studies. On an inbred genetic background our study observed the congenital OFT defect DORV for the first time in *Smad6* mutants. During this time, another group showed that in zebrafish *Smad6* is required to down regulate BMP signaling in cardiac-progenitors as they differentiate into cardiomyocytes of the elongating OFT (de Pater et al., 2012). In mice, disruption of SHF-dependant OFT elongation and the subsequent maturation of cardiomyocytes within the truncus have been linked to several types of congenital defects including DORV (Ward and Kirby, 2006). Our data shows mRNA expression of *Smad6* within the distal myocardial layer of the developing OFT, raising the possibility that *Smad6* serves a conserved role in differentiation of the anterior SHF. However, direct evidence for this has yet to be investigated. To investigate this, expression of progenitor markers, such as Isl1, could be examined in *Smad6* mutant OFT myocardium. Also mutants may exhibit morphological differences in the angle and length of the OFT during SHF migration.

Another interesting avenue of further research would be investigating whether Smad6 is involved in hematopoietic emergence from the endocardium. Our group has recently published the first description of 'hemogenic endocardium' within the heart (Nakano et al., 2013), but little is functionally known about the molecular mechanism of this process. Interestingly, hematopoiesis within the heart is restricted to the same specialized subset of cushion endocarium that are involved in valve formation. Further, hemogenic activity within the endocaridum occurs at the same time as EMT. Given this correlation it stands to reason that some of the same mechanisms that result in the down regulation of endothelial specific genes and the activation of EMT could be shared in the process of switching from an endothelial gene program to a hematopoietic one. Our data already shows that *Smad6* is expressed within the correct location at the right time, while other work shows that *Smad6* is linked to the genetic regulation of key hematopoietic genes (Knezevic et al., 2011). Interestingly, *Smad6* is also expressed within the dorsal aorta (Galvin et al., 2000) allowing for convenient internal comparison of any phenotypes within the heart to another hematopoietic tissue.

Clinical Implications

Aortic Dissection

Aortic dissection is a potentially lethal cardiac condition with 6000-10,000 cases occurring within the United States each year (Suzuki et al., 2003; Hagan et al., 2000). While incidence is generally correlated to age, evidence suggests that the number of cases is rising at a rate that surpasses an increase based solely on an ageing population (Nienaber et al., 2005). Distinct differences in the severity and treatment of dissections exist depending on the site of origin. Dissections originating within the cardiac progenitor-derived ascending aorta (DeBakey Type

I/II, Stanford Type A) require surgery and carry a higher death rate than dissections originating in the descending aorta (DeBakey Type III, Stanford Type B) (Hagan et al., 2000; Hiratzka et al., 2010). Aortic dissection is triggered by a tear within the intima (endothelial layer) that allows blood to create and occupy a false lumen within the aortic wall (Nienaber and Powell, 2012; Braverman, 2011). The creation of an endothelial tear is preceded by the degeneration of aortic smooth muscle (Nienaber and Powell, 2012), highlighting the importance of smooth muscle integrity within the aortic region.

Endocardial Cushion Defects

Congenital heart defects are the most common of all birth defects taking place in 1% of live births (Hoffman, 1990). Of these heart defects, the majority is associated with the improper formation of the endocardial cushions and the tissue derived from the cushion mesenchyme (Samánek et al., 1989). Within the developing heart the cushion msenschyme is responsible for the many aspects of cardiac remodeling and morphogenesis. Malformation of the endocardial cushions can result in variety of pathologies including: atrial septal defect (ASD), ventricular septal defect (VSD), atrioventricular canal (AV canal), outflow tract misalignment and valve malformations. Valve malformations, specifically, constitute almost a third of congenital cardiac malformations (Hoffman, 1990; Samánek et al., 1989) and valve replacement procedures represent one of the most common cardiac surgeries within the United States (Roberts and Ko, 2005). Valves that require replacement are commonly associated with congenital malformations (Supino et al., 2004), emphasizing the importance of understanding the molecular basis of valve formation within development.

REFERENCES

Brade, T., Pane, L.S., Moretti, A., Chien, K.R., and Laugwitz, K.L. 2013. Embryonic heart progenitors and cardiogenesis. *Cold Spring Harb Perspect Med* **3:**a013847.

Braverman, A.C. 2011. Aortic dissection: Prompt diagnosis and emergency treatment are critical. *Cleve Clin J Med* **78:**685-696.

Cai, C.L., Liang, X., Shi, Y., Chu, P.H., Pfaff, S.L., Chen, J., and Evans, S. 2003. Isl1 identifies a cardiac progenitor population that proliferates prior to differentiation and contributes a majority of cells to the heart. *Dev Cell* **5:**877-889.

Camenisch, T.D., Molin, D.G., Person, A., Runyan, R.B., Gittenberger-de Groot, A.C., McDonald, J.A., and Klewer, S.E. 2002. Temporal and distinct TGFbeta ligand requirements during mouse and avian endocardial cushion morphogenesis. *Dev Biol* **248:**170-181.

Chen, Q., Chen, H., Zheng, D., Kuang, C., Fang, H., Zou, B., Zhu, W., Bu, G., Jin, T., Wang, Z., Zhang, X., Chen, J., Field, L.J., Rubart, M., Shou, W., and Chen, Y. 2009. Smad7 is required for the development and function of the heart. *J Biol Chem* **284:**292-300.

Cheung, C., Bernardo, A.S., Trotter, M.W., Pedersen, R.A., and Sinha, S. 2012. Generation of human vascular smooth muscle subtypes provides insight into embryological origin-dependent disease susceptibility. *Nat Biotechnol* **30:**165-173.

Del Monte, G., and Harvey, R.P. 2012. An endothelial contribution to coronary vessels. *Cell* **151:**932-934.

Dickson, M.C., Slager, H.G., Duffie, E., Mummery, C.L., and Akhurst, R.J. 1993. RNA and protein localisations of TGF beta 2 in the early mouse embryo suggest an involvement in cardiac development. *Development* **117:**625-639.

Du, K.L., Ip, H.S., Li, J., Chen, M., Dandre, F., Yu, W., Lu, M.M., Owens, G.K., and Parmacek, M.S. 2003. Myocardin is a critical serum response factor cofactor in the transcriptional program regulating smooth muscle cell differentiation. *Mol Cell Biol* **23:**2425-2437.

Dudley, A.T., and Robertson, E.J. 1997. Overlapping expression domains of bone morphogenetic protein family members potentially account for limited tissue defects in BMP7 deficient embryos. *Dev Dyn* **208:**349-362.

Faugeroux, J., Nematalla, H., Li, W., Clement, M., Robidel, E., Frank, M., Curis, E., Ait-Oufella, H., Caligiuri, G., Nicoletti, A., Hagege, A., Messas, E., Bruneval, P., Jeunemaitre, X., and Bergaya, S. 2013. Angiotensin II promotes thoracic aortic dissections and ruptures in Col3a1 haploinsufficient mice. *Hypertension* **62:**203-208.

Galvin, K.M., Donovan, M.J., Lynch, C.A., Meyer, R.I., Paul, R.J., Lorenz, J.N., Fairchild-Huntress, V., Dixon, K.L., Dunmore, J.H., Gimbrone, M.A., Falb, D., and Huszar, D. 2000. A role for smad6 in development and homeostasis of the cardiovascular system. *Nat Genet* **24:**171-174.

Gong, B., Trent, M.B., Srivastava, D., and Boor, P.J. 2006. Chemical-induced, nonlethal, developmental model of dissecting aortic aneurysm. *Birth Defects Res A Clin Mol Teratol* **76:**29-38.

Hagan, P.G., Nienaber, C.A., Isselbacher, E.M., Bruckman, D., Karavite, D.J., Russman, P.L., Evangelista, A., Fattori, R., Suzuki, T., Oh, J.K., Moore, A.G., Malouf, J.F., Pape, L.A., Gaca, C., Sechtem, U., Lenferink, S., Deutsch, H.J., Diedrichs, H., Marcos y Robles, J., Llovet, A., Gilon, D., Das, S.K., Armstrong, W.F., Deeb, G.M., and Eagle, K.A. 2000. The International Registry of Acute Aortic Dissection (IRAD): new insights into an old disease. *JAMA* **283:**897-903.

Harmon, Andrew W and Atsushi Nakano. *Genesis*. United States: 2013.

Hata, A., Lagna, G., Massagué, J., and Hemmati-Brivanlou, A. 1998. Smad6 inhibits BMP/Smad1 signaling by specifically competing with the Smad4 tumor suppressor. *Genes Dev* **12:**186-197.

Hayashi, H., Abdollah, S., Qiu, Y., Cai, J., Xu, Y.Y., Grinnell, B.W., Richardson, M.A., Topper, J.N., Gimbrone, M.A., Wrana, J.L., and Falb, D. 1997. The MAD-related protein Smad7 associates with the TGFbeta receptor and functions as an antagonist of TGFbeta signaling. *Cell* **89:**1165-1173.

Hiratzka, L.F., Bakris, G.L., Beckman, J.A., Bersin, R.M., Carr, V.F., Casey, D.E., Eagle, K.A., Hermann, L.K., Isselbacher, E.M., Kazerooni, E.A., Kouchoukos, N.T., Lytle, B.W., Milewicz, D.M., Reich, D.L., Sen, S., Shinn, J.A., Svensson, L.G., Williams, D.M., and Society for Vascular Medicine. 2010. 2010 ACCF/AHA/AATS/ACR/ASA/SCA/SCAI/SIR/STS/SVM guidelines for the diagnosis and management of patients with thoracic aortic disease: executive summary. A report of the American College of Cardiology Foundation/American Heart Association Task Force on Practice Guidelines, American Association for Thoracic Surgery, American College of Radiology, American Stroke Association, Society of Cardiovascular Anesthesiologists, Society for Cardiovascular Angiography and Interventions, Society of Interventional Radiology, Society of Thoracic Surgeons, and Society for Vascular Medicine. *Catheter Cardiovasc Interv* **76:**E43-E86.

Hoffman, J.I. 1990. Congenital heart disease: incidence and inheritance. *Pediatric Clinics of North America* **37:**25-43.

Hoofnagle, M.H., Neppl, R.L., Berzin, E.L., Teg Pipes, G.C., Olson, E.N., Wamhoff, B.W., Somlyo, A.V., and Owens, G.K. 2011. Myocardin is differentially required for the development of smooth muscle cells and cardiomyocytes. *Am J Physiol Heart Circ Physiol* **300:**H1707-H1721.

Huang, J., Cheng, L., Li, J., Chen, M., Zhou, D., Lu, M.M., Proweller, A., Epstein, J.A., and Parmacek, M.S. 2008. Myocardin regulates expression of contractile genes in smooth muscle cells and is required for closure of the ductus arteriosus in mice. *J Clin Invest* **118:**515-525.

Huang, J., Elicker, J., Bowens, N., Liu, X., Cheng, L., Cappola, T.P., Zhu, X., and Parmacek, M.S. 2012. Myocardin regulates BMP10 expression and is required for heart development. *J Clin Invest* **122:**3678-3691.

Huang, J., Min Lu, M., Cheng, L., Yuan, L.J., Zhu, X., Stout, A.L., Chen, M., Li, J., and Parmacek, M.S. 2009. Myocardin is required for cardiomyocyte survival and maintenance of heart function. *Proc Natl Acad Sci U S A* **106:**18734-18739.

Imamura, T., Takase, M., Nishihara, A., Oeda, E., Hanai, J., Kawabata, M., and Miyazono, K. 1997. Smad6 inhibits signalling by the TGF-beta superfamily. *Nature* **389:**622-626.

Jiang, X., Rowitch, D.H., Soriano, P., McMahon, A.P., and Sucov, H.M. 2000. Fate of the mammalian cardiac neural crest. *Development* **127:**1607-1616.

Jiao, K., Kulessa, H., Tompkins, K., Zhou, Y., Batts, L., Baldwin, H.S., and Hogan, B.L. 2003. An essential role of Bmp4 in the atrioventricular septation of the mouse heart. *Genes Dev* **17:**2362-2367.

Kattman, S.J., Huber, T.L., and Keller, G.M. 2006. Multipotent flk-1+ cardiovascular progenitor cells give rise to the cardiomyocyte, endothelial, and vascular smooth muscle lineages. *Dev Cell* **11:**723-732.

Kelly, R.G., Brown, N.A., and Buckingham, M.E. 2001. The arterial pole of the mouse heart forms from Fgf10-expressing cells in pharyngeal mesoderm. *Dev Cell* **1:**435-440.

Kim, R.Y., Robertson, E.J., and Solloway, M.J. 2001. Bmp6 and Bmp7 are required for cushion formation and septation in the developing mouse heart. *Dev Biol* **235:**449-466.

Knezevic, K., Bee, T., Wilson, N.K., Janes, M.E., Kinston, S., Polderdijk, S., Kolb-Kokocinski, A., Ottersbach, K., Pencovich, N., Groner, Y., de Bruijn, M., Göttgens, B., and Pimanda, J.E. 2011. A Runx1-Smad6 rheostat controls Runx1 activity during embryonic hematopoiesis. *Mol Cell Biol* **31:**2817-2826.

Komiyama, M., Ito, K., and Shimada, Y. 1987. Origin and development of the epicardium in the mouse embryo. *Anat Embryol (Berl)* **176:**183-189.

Krug, E.L., Mjaatvedt, C.H., and Markwald, R.R. 1987. Extracellular matrix from embryonic myocardium elicits an early morphogenetic event in cardiac endothelial differentiation. *Dev Biol* **120:**348-355.

Li, J., Zhu, X., Chen, M., Cheng, L., Zhou, D., Lu, M.M., Du, K., Epstein, J.A., and Parmacek, M.S. 2005. Myocardin-related transcription factor B is required in cardiac neural crest for smooth muscle differentiation and cardiovascular development. *Proc Natl Acad Sci U S A* **102:**8916-8921.

Li, S., Wang, D.Z., Wang, Z., Richardson, J.A., and Olson, E.N. 2003. The serum response factor coactivator myocardin is required for vascular smooth muscle development. *Proc Natl Acad Sci U S A* **100:**9366-9370.

Liebman, J. 1976. Congenital Malformations of the Heart: Embryology, Anatomy, and Operative Considerations. *JAMA: The Journal of the American Medical Association* **236:**1752-1752.

Lluri, G., and Aboulhosn, J. 2014. Coronary Arterial Development: A Review of Normal and Congenitally Anomalous Patterns. *Clin Cardiol* .

Lyons, K.M., Pelton, R.W., and Hogan, B.L. 1990. Organogenesis and pattern formation in the mouse: RNA distribution patterns suggest a role for bone morphogenetic protein-2A (BMP-2A). *Development* **109:**833-844.

MacLennan, D.H., Brandl, C.J., Korczak, B., and Green, N.M. 1985. Amino-acid sequence of a Ca2+ + Mg2+-dependent ATPase from rabbit muscle sarcoplasmic reticulum, deduced from its complementary DNA sequence. *Nature* **316:**696-700.

Majesky, M.W. 2007. Developmental basis of vascular smooth muscle diversity. *Arterioscler Thromb Vasc Biol* **27:**1248-1258.

Manasek, F.J. 1976. Heart development: interactions involved in cardiac morphogenesis. *Cell surface reviews* **1976:**.

Martin-Puig, S., Wang, Z., and Chien, K.R. 2008. Lives of a heart cell: tracing the origins of cardiac progenitors. *Cell Stem Cell* **2:**320-331.

Massagué, J., Seoane, J., and Wotton, D. 2005. Smad transcription factors. *Genes Dev* **19:**2783-2810.

Männer, J. 2000. Cardiac looping in the chick embryo: a morphological review with special reference to terminological and biomechanical aspects of the looping process. *Anat Rec* **259:**248-262.

McCulley, D.J., Kang, J.O., Martin, J.F., and Black, B.L. 2008. BMP4 is required in the anterior heart field and its derivatives for endocardial cushion remodeling, outflow tract septation, and semilunar valve development. *Dev Dyn* **237:**3200-3209.

Miano, J.M. 2003. Serum response factor: toggling between disparate programs of gene expression. *J Mol Cell Cardiol* **35:**577-593.

Mikawa, T., and Gourdie, R.G. 1996. Pericardial mesoderm generates a population of coronary smooth muscle cells migrating into the heart along with ingrowth of the epicardial organ. *Dev Biol* **174:**221-232.

Mjaatvedt, C.H., Lepera, R.C., and Markwald, R.R. 1987. Myocardial specificity for initiating endothelial-mesenchymal cell transition in embryonic chick heart correlates with a particulate distribution of fibronectin. *Dev Biol* **119:**59-67.

Moorman, A.F., Christoffels, V.M., Anderson, R.H., and van den Hoff, M.J. 2007. The heart-forming fields: one or multiple? *Philosophical Transactions of the Royal Society B: Biological Sciences* **362:**1257-1265.

Moretti, A., Caron, L., Nakano, A., Lam, J.T., Bernshausen, A., Chen, Y., Qyang, Y., Bu, L., Sasaki, M., Martin-Puig, S., Sun, Y., Evans, S.M., Laugwitz, K.L., and Chien, K.R. 2006. Multipotent embryonic isl1+ progenitor cells lead to cardiac, smooth muscle, and endothelial cell diversification. *Cell* **127:**1151-1165.

Morrow, D., Guha, S., Sweeney, C., Birney, Y., Walshe, T., OBrien, C., Walls, D., Redmond, E.M., and Cahill, P.A. 2008. Notch and vascular smooth muscle cell phenotype. *Circ Res* **103:**1370-1382.

Moses, K.A., DeMayo, F., Braun, R.M., Reecy, J.L., and Schwartz, R.J. 2001. Embryonic expression of an Nkx2-5/Cre gene using ROSA26 reporter mice. *Genesis* **31:**176-180.

Moustakas, A., Souchelnytskyi, S., and Heldin, C.-H. 2001. Smad regulation in TGF-β signal transduction. *Journal of Cell Science* **114:**4359-4369.

Nakano, A., Nakano H., and Chien K.R. 2008 Multipotent Isl+ cardiovascular progenitors in development and disease. Cold Spring Harb Symp Quant Biol **73**:297-306.

Nakano, H., Liu, X., Arshi, A., Nakashima, Y., van Handel, B., Sasidharan, R., Harmon, A.W., Shin, J.H., Schwartz, R.J., Conway, S.J., Harvey, R.P., Pashmforoush, M., Mikkola, H.K., and Nakano, A. 2013. Haemogenic endocardium contributes to transient definitive haematopoiesis. *Nat Commun* **4:**1564.

Nakano, H., Williams, E., Hoshijima, M., Sasaki, M., Minamisawa, S., Chien, K.R., and Nakano, A. 2011. Cardiac origin of smooth muscle cells in the inflow tract. *J Mol Cell Cardiol* **50:**337-345.

Nakao, A., Afrakhte, M., Morén, A., Nakayama, T., Christian, J.L., Heuchel, R., Itoh, S., Kawabata, M., Heldin, N.E., Heldin, C.H., and ten Dijke, P. 1997. Identification of Smad7, a TGFbeta-inducible antagonist of TGF-beta signalling. *Nature* **389:**631-635.

Nakayama, T., Gardner, H., Berg, L.K., and Christian, J.L. 1998. Smad6 functions as an intracellular antagonist of some TGF-beta family members during Xenopus embryogenesis. *Genes Cells* **3:**387-394.

Nienaber, C.A., and Powell, J.T. 2012. Management of acute aortic syndromes. *Eur Heart J* **33:**26-35b.

Nienaber, C.A., Zannetti, S., Barbieri, B., Kische, S., Schareck, W., and Rehders, T.C. 2005. INvestigation of STEnt grafts in patients with type B Aortic Dissection: design of the INSTEAD trial—a prospective, multicenter, European randomized trial. *Am Heart J* **149:**592-599.

Norman, C., Runswick, M., Pollock, R., and Treisman, R. 1988. Isolation and properties of cDNA clones encoding SRF, a transcription factor that binds to the c-fos serum response element. *Cell* **55:**989-1003.

de Pater, E., Ciampricotti, M., Priller, F., Veerkamp, J., Strate, I., Smith, K., Lagendijk, A.K., Schilling, T.F., Herzog, W., Abdelilah-Seyfried, S., Hammerschmidt, M., and Bakkers, J. 2012. Bmp signaling exerts opposite effects on cardiac differentiation. *Circ Res* **110:**578-587.

PATTEN, B.M., KRAMER, T.C., and BARRY, A. 1948. Valvular action in the embryonic chick heart by localized apposition of endocardial masses. *Anat Rec* **102:**299-311.

Pearson, C.A., Ohyama, K., Manning, L., Aghamohammadzadeh, S., Sang, H., and Placzek, M. 2011. FGF-dependent midline-derived progenitor cells in hypothalamic infundibular development. *Development* **138:**2613-2624.

Pérez-Pomares, J.M., Carmona, R., González-Iriarte, M., Atencia, G., Wessels, A., and Muñoz-Chápuli, R. 2002. Origin of coronary endothelial cells from epicardial mesothelium in avian embryos. *Int J Dev Biol* **46:**1005-1013.

Potts, J.D., and Runyan, R.B. 1989. Epithelial-mesenchymal cell transformation in the embryonic heart can be mediated, in part, by transforming growth factor β. *Dev Biol* **134:**392-401.

Red-Horse, K., Ueno, H., Weissman, I.L., and Krasnow, M.A. 2010. Coronary arteries form by developmental reprogramming of venous cells. *Nature* **464:**549-553.

Roberts, W.C., and Ko, J.M. 2005. Frequency by decades of unicuspid, bicuspid, and tricuspid aortic valves in adults having isolated aortic valve replacement for aortic stenosis, with or without associated aortic regurgitation. *Circulation* **111:**920-925.

Runyan, R.B., and Markwald, R.R. 1983. Invasion of mesenchyme into three-dimensional collagen gels: a regional and temporal analysis of interaction in embryonic heart tissue. *Dev Biol* **95:**108-114.

Saga, Y., Miyagawa-Tomita, S., Takagi, A., Kitajima, S., Miyazaki, J.i., and Inoue, T. 1999. MesP1 is expressed in the heart precursor cells and required for the formation of a single heart tube. *Development* **126:**3437-3447.

Samánek, M., Slavík, Z., Zborilová, B., Hrobonová, V., Voríšková, M., and Skovránek, J. 1989. Prevalence, treatment, and outcome of heart disease in live-born children: a prospective analysis of 91,823 live-born children. *Pediatr Cardiol* **10:**205-211.

Sanford, L.P., Ormsby, I., Gittenberger-de Groot, A.C., Sariola, H., Friedman, R., Boivin, G.P., Cardell, E.L., and Doetschman, T. 1997. TGFbeta2 knockout mice have multiple developmental defects that are non-overlapping with other TGFbeta knockout phenotypes. *Development* **124:**2659-2670.

Shi, Y., and Massagué, J. 2003. Mechanisms of TGF-β signaling from cell membrane to the nucleus. *Cell* **113:**685-700.

Showell, C., Binder, O., and Conlon, F.L. 2004. T-box genes in early embryogenesis. *Dev Dyn* **229:**201-218.

Snider, P., Tang, S., Lin, G., Wang, J., and Conway, S.J. 2009. Generation of Smad7-Cre recombinase mice: A useful tool for the study of epithelial-mesenchymal transformation within the embryonic heart. *Genesis* **47:**469-475.

Solloway, M.J., and Robertson, E.J. 1999. Early embryonic lethality in Bmp5;Bmp7 double mutant mice suggests functional redundancy within the 60A subgroup. *Development* **126:**1753-1768.

Sugi, Y., Yamamura, H., Okagawa, H., and Markwald, R.R. 2004. Bone morphogenetic protein-2 can mediate myocardial regulation of atrioventricular cushion mesenchymal cell formation in mice. *Dev Biol* **269:**505-518.

Sun, Y., Liang, X., Najafi, N., Cass, M., Lin, L., Cai, C.L., Chen, J., and Evans, S.M. 2007. Islet 1 is expressed in distinct cardiovascular lineages, including pacemaker and coronary vascular cells. *Dev Biol* **304:**286-296.

Supino, P.G., Borer, J.S., Yin, A., Dillingham, E., and McClymont, W. 2004. The epidemiology of valvular heart diseases: the problem is growing. *Adv Cardiol* **41:**9-15.

Suzuki, T., Mehta, R.H., Ince, H., Nagai, R., Sakomura, Y., Weber, F., Sumiyoshi, T., Bossone, E., Trimarchi, S., Cooper, J.V., Smith, D.E., Isselbacher, E.M., Eagle, K.A., Nienaber, C.A., and International Registry of Aortic Dissection. 2003. Clinical profiles and outcomes of acute type B aortic dissection in the current era: lessons from the International Registry of Aortic Dissection (IRAD). *Circulation* **108 Suppl 1:**II312-II317.

Taber, L.A., Lin, I., and Clark, E.B. 1995. Mechanics of cardiac looping. *Developmental dynamics* **203:**42-50.

Tanigaki, K., Han, H., Yamamoto, N., Tashiro, K., Ikegawa, M., Kuroda, K., Suzuki, A., Nakano, T., and Honjo, T. 2002. Notch-RBP-J signaling is involved in cell fate determination of marginal zone B cells. *Nat Immunol* **3:**443-450.

Topouzis, S., and Majesky, M.W. 1996. Smooth muscle lineage diversity in the chick embryo. Two types of aortic smooth muscle cell differ in growth and receptor-mediated transcriptional responses to transforming growth factor-beta. *Dev Biol* **178:**430-445.

van den Berg, G., Abu-Issa, R., de Boer, B.A., Hutson, M.R., de Boer, P.A., Soufan, A.T., Ruijter, J.M., Kirby, M.L., van den Hoff, M.J., and Moorman, A.F. 2009. A caudal proliferating growth center contributes to both poles of the forming heart tube. *Circ Res* **104:**179-188.

Verzi, M.P., McCulley, D.J., De Val, S., Dodou, E., and Black, B.L. 2005. The right ventricle, outflow tract, and ventricular septum comprise a restricted expression domain within the secondary/anterior heart field. *Dev Biol* **287:**134-145.

Waldo, K.L., Hutson, M.R., Ward, C.C., Zdanowicz, M., Stadt, H.A., Kumiski, D., Abu-Issa, R., and Kirby, M.L. 2005. Secondary heart field contributes myocardium and smooth muscle to the arterial pole of the developing heart. *Dev Biol* **281:**78-90.

Wang, Z., Wang, D.-Z., Pipes, G.C.T., and Olson, E.N. 2003. Myocardin is a master regulator of smooth muscle gene expression. *Proceedings of the National Academy of Sciences* **100:**7129-7134.

Ward, C., and Kirby, M. 2006. The secondary heart field: understanding conotruncal defects from a developmental perspective. *Current Cardiology Reviews* **2:**65-69.

Wu, B., Zhang, Z., Lui, W., Chen, X., Wang, Y., Chamberlain, A.A., Moreno-Rodriguez, R.A., Markwald, R.R., O'Rourke, B.P., Sharp, D.J., Zheng, D., Lenz, J., Baldwin, H.S., Chang, C.P., and Zhou, B. 2012. Endocardial cells form the coronary arteries by angiogenesis through myocardial-endocardial VEGF signaling. *Cell* **151:**1083-1096.

Wu, S.M., Fujiwara, Y., Cibulsky, S.M., Clapham, D.E., Lien, C.L., Schultheiss, T.M., and Orkin, S.H. 2006. Developmental origin of a bipotential myocardial and smooth muscle cell precursor in the mammalian heart. *Cell* **127:**1137-1150.

Yamada, M., Szendro, P.I., Prokscha, A., Schwartz, R.J., and Eichele, G. 1999. Evidence for a role of Smad6 in chick cardiac development. *Dev Biol* **215:**48-61.

Yang, X., Dormann, D., Münsterberg, A.E., and Weijer, C.J. 2002. Cell movement patterns during gastrulation in the chick are controlled by positive and negative chemotaxis mediated by FGF4 and FGF8. *Dev Cell* **3:**425-437.

Zaffran, S., Kelly, R.G., Meilhac, S.M., Buckingham, M.E., and Brown, N.A. 2004. Right ventricular myocardium derives from the anterior heart field. *Circ Res* **95:**261-268.

Zhou, B., von Gise, A., Ma, Q., Rivera-Feliciano, J., and Pu, W.T. 2008. Nkx2-5- and Isl1-expressing cardiac progenitors contribute to proepicardium. *Biochem Biophys Res Commun* **375:**450-453.